2013

Pure Component Adsorption of Methane, Ethylene, Propylene and Carbon Dioxide in Silicalite

Qianqian Zhou
Cleveland State University

PURE COMPONENT ADSORPTION OF METHANE, ETHYLENE, PROPYLENE AND CARBON DIOXIDE IN SILICALITE

QIANQIAN ZHOU

Bachelor of Science in Chemical Engineering and Technology

Chongqing University

June 2010

submitted in partial fulfillment of requirements for the degree

MASTER OF SCIENCE IN CHEMICAL ENGINEERING

at the

CLEVELAND STATE UNIVERSITY

May 2013

This thesis has been approved

for the Department of CHEMICAL and BIOMEDICAL ENGINEERING

and the College of Graduate Studies by

_____

Thesis Committee Chairperson, Dr. Orhan Talu

_____

Department & Date

_____

Dr. Dhananjai B. Shah

_____

Chair, Department & Date

_____

Dr. Chandra Kothapalli

_____

Department & Date

ACKNOWLEDGEMENTS

I wish to express my sincere gratitude to my advisor, Dr. Talu, for his support and guidance throughout my thesis writing. This thesis could not be possible without his patience, motivation and immense knowledge. His effort and input in this work are invaluable.

Acknowledgements are also extended to the rest of my thesis committee, Dr. Shah and Dr. Kothapalli for their insightful comments and evaluating of this work. I would like to thank Dr. Shah for his advice on several technical issues. My sincere thanks go to Dr. Shah and Dr. Talu, for offering me the assistant opportunities which provided me financial support in the past two years.

I owe thankfulness to Dr. Gatica who inspired me in writing the Matlab program. Thank you for always making time in your busy agenda to talk about new ideas, to take a quick look at my program and provided modifications.

It is a great pleasure to thank everyone who helped me write my thesis successfully. I am obliged to many of my friends who supported me spiritually throughout my study abroad.

Last but not the least, I would like to thank my parents, for giving birth to me at the first place and always believing in me and supportive for my studies. I am so lucky to have you in my life.

PURE COMPONENT ADSORPTION OF METHANE, ETHYLENE, PROPYLENE AND CARBON DIOXIDE IN SILICALITE

QIANQIAN ZHOU

ABSTRACT

Adsorption isotherms are measured for pure methane, ethylene, propylene and carbon dioxide in silicalite. Isotherm data are collected using a volumetric method at three different temperatures of 10C, 35C and 65C at pressure up to 100psi. The Virial equation and Langmuir equation have been applied to represent excess amount adsorbed in each pure component system. The binary adsorption equilibrium for various mixtures are predicted from the pure component adsorption data, using the Ideal Adsorption Solution Theory (IAST).

Table of Contents

LIST OF FIGURES

LIST OF TABLES

NOMENCLATURE

A specific surface area, total surface area of a material per unit of mass ($cm^2/gram\ solid$)

a molar surface area ($cm^2/mole\ adsorbed$)

K Henry's Law constant

m_s the activated mass of solid which is independently measured.

N number of moles

N_i the number of moles of fluid component i in adsorbed phase

n_i the component i amount adsorbed per unit of solid mass, $n_i = N_i/m_s$

P equilibrium pressure

R universal gas constant, (8.314472 J/(mol·K))

Greek Symbols

π spreading pressure

μ_s the chemical potential of species i (same in the fluid and adsorbed phase).

μ_s^* the chemical potential of pure solid without adsorbed phase.

CHAPTER I

INTRODUCTION

Principles of Adsorption

The term adsorption was first introduced by Kayser (1881) to explain the condensation of gases on solid surface, in which the solid is considered impenetrable. Adsorption is defined as the enrichment of one or more components from a fluid phase in the interfacial layer between two bulk phases, such as a solid and a gas. The solid is called the adsorbent, while gas is called the adsorbate. Different components of a gas stream can be selectively collected and concentrated onto a solid surface by tailoring solid properties, the selectivity can be manipulated. Therefore, adsorption can be uniquely advantageous compared to other bulk separation methods where selectivity is fixed by the nature of fluid components [1].

Adsorption process has been extensively used in purification processes and bulk separation processes. The process is called purification process, if only trace contaminants from the process stream need to be removed. Purification of gases by adsorption is in widespread used in air pollution control. Application of adsorption for waste water treatment is also well known application. Adsorption processes are classified as bulk separation processes, if one component needs to be recovered selectively from a mixture in high concentrations, such as, nitrogen or oxygen production from air, hydrogen production from reformer gas, ethanol production from fermentation broth, etc.

Solid: silicalite

Adsorption, a heavily materials-driven technology, has been well developed along with the development of microporous adsorbents such as silica gel, activated carbon, alumina and zeolites (sometimes called molecular sieves).

Zeolites are porous crystalline aluminosilicates. The zeolite framework consists of an assemblage of tetrahedrons (classically, SiO4 or AlO4), joined together in various regular arrays through shared oxygen atoms, to form an open crystal lattice [2]. A tetrahedron is composed of a metal cation at the center and oxygen anions at the four apexes. For example, a silicate tetrahedron is sketched in Figure 1.1. The silicon atom is bonded to four oxygen atoms. Its valence is satisfied but each oxygen has only half of its charge

satisfied, therefore can form a bond with another silicon atom to join tetrahedrons in three dimensions. There are numerous different ways to stack the tetrahedrons and hundreds of unique framework structures resulting from different combinations are known [11].

Figure 1.1 Silicate Tetrahedron (From 'Wikipedia Commons')

Aluminum plays an important role in silicate structures. The ionic radii of Al makes it easily fit into a tetrahedral instead of Si. If Si tetrahedral site is occupied by Al, the substitution results in a net negative charge since Al is +3 and Si is +4. The negative charge is balanced by an ionized bonded cation in the immediate vicinity of Al site. As a result, along with Al/Si ratio of a zeolite increase, the cation content increase and its surface selectivity changes from hydrophobic to hydrophilic. The cations can be ion-exchanged with others in a solution which enables tailoring of the zeolite structure for specific purposes. Cation exchange can result in charges in the sites of porous network as well as changes in the surface potential. As a side effect the chemical and thermal stability of zeolites decrease with increasing Al content.

Silicalite used in the study is the aluminum-free form of zeolite MFI (or ZSM-5). It has both straight elliptical channels and zigzag channels that cross at the intersections. The three-dimensional interconnected channels are 10-member oxygen rings of free diameter about 5.6 Å, which are intermediate between the small-port sieves with 8-ring channels(e.g. LTA or zeolite-A) and the large-port sieves with 12-ring channels[2](e.g. FAU or zeolite-X and Y). The channel systems of silicalite and a characteristic complex of 10-rings are sketched in Figure 1.1.

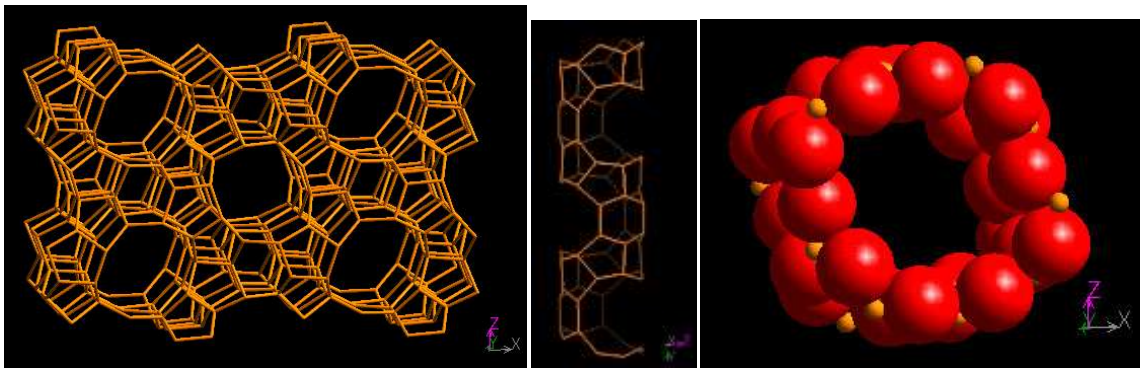

Figure 1.2 Framework Type MFI, 10-ring straight channel and complex of 10-rings viewed along b-axis (From 'Database of Zeolite Structures')

Silicalite is hydrophobic in nature and has no ion exchange capacity since it does not contain any Al atoms. It is characterized by great thermal and chemical stability. Its surface has been considered as homogeneous. However, a heterogeneous behavior may

also exhibited without any cations in the pore structure because of geometric effects, due to different adsorbates located at different sites in the silicalite [3].

Scope of work

Pure component adsorption isotherm is the most basic/fundamental characteristic of adsorption equilibrium. It is the equilibrium relation between the amount of the adsorbed substance and the pressure in the bulk fluid phase at constant temperature.

A better understanding of mixture equilibrium behavior in adsorbents is important for the optimization of adsorption separation processes. However, experimental measurements of the multi-component adsorption isotherm are time-consuming and complicated because of the additional degree of freedom i.e. bulk composition. As a consequence experimental data are scarce. In present work, the binary adsorption equilibrium for various mixtures are predicted from the pure component adsorption data, using the Ideal Adsorption Solution Theory (IAST). As the name implies, IAST assumes an ideal mixture of components in the adsorbed phase.

The pure component isotherm data as points cannot be conveniently used to calculate IAST results for mixtures. Thus, the pure component isotherm data is correlated with appropriate isotherm equations to facilitate the computations.

The primary purpose of this study is to collect isotherm data for several gases (i.e. methane, ethylene, propylene and CO2) at numerous temperatures (i.e. 10C, 35C, 65C) in silicalite. Experimental isotherm data are then correlated with isotherm equations and mixture (only binary) equilibrium behavior are predicted using IAST.

CHAPTER II

THEORY

Excess adsorption and Gibbs isotherm adsorption

Excess adsorption is the number of molecules in micropores in excess of the amount that would be actually present in the ambient bulk fluid phase. Excess adsorption can be measured in experiment which is different from the absolute adsorption, the actual number of molecules in micropores. The difference between absolute and excess adsorption is negligible at the sub-atmospheric pressure [12].

The absolute amount adsorbed, based on a unit surface area is the integral of density profile normal to a surface (Talu and Myers, 2001) as,

$$\Gamma^{abs} = \int_0^L \rho(z)\, dz \qquad (2\text{-}1)$$

Where $\rho(z)$ is local density and z is distance perpendicular to a surface. The limits of the interfacial region, however, are very difficult to define. In this equation the upper limit for integration L is a function of T&P which complicate the use of this definition.

As the first person to realize this complication, Gibbs (1928) introduced the concept of a "dividing surface" between two bulk phases. This hypothetical surface clearly separates the ill-defined interfacial region into two distinct phases. Also, he assumed that the fluid phase and impenetrable solid phase have uniform properties.

Compared to the actual adsorption condition, the changes in properties are attributed to a two-dimensional adsorbed phase, the dividing surface. All the general properties except volume are called "Gibbs surface excess". The adsorbed phase does not have a volume since it is two-dimensional. The surface excess adsorption with Gibbs definition is

$$\Gamma^{ex} = \int_{z_0}^{\infty} (\rho\{z\} - \rho^g)\, dz \qquad (2\text{-}2)$$

This expression overcomes the ambiguity caused by the unclear upper limit of integration L in Eq. (2-1). The low integration limit z_0 corresponds to where the Gibbs dividing surface is located, which is not explained in Gibbs original work. Location of z_0 determines the reference state in adsorption thermodynamics.

When it comes to the microporous adsorbent, most of the concepts of adsorption developed from flat surfaces are no longer valid, such as Langmuir and BET formulation. This is because the surface area of the porous solid cannot be independently measured

without any adsorption. Surface area loses its physical significance and cannot be used as the extensive thermodynamic property. (Gumma and Talu,2010)

As a surface area- independent definition, the Gibbs dividing surface can be extended from flat surfaces to porous solids, as long as a reference state (which is independent of the system properties such as T and P) is used to locate the dividing surface. Then the Eq.(2-2) is only a definition of an excess thermodynamic property.(Talu, 2010)

Gibbs definition of adsorption is a mathematical description and does not imply any shape of the surface phase. The fundamental property relation for the total internal energy U for adsorbed phase as (Talu, 2010)

$$dU = T\,dS - P\,dV + \sum \mu_i dN_i + \left(\mu_s - \mu_s^*\right)dm_s \qquad (2\text{-}3)$$

μ_s^* is the chemical potential of pure solid without adsorbed phase. μ_s is the chemical potential of species i (same in the fluid and adsorbed phase). N_i is the number of moles of fluid component i in adsorbed phase. S is the entropy for the adsorbed phase. m_s is the activated mass of solid which is independently measured.

The $P\,dV$ term can be neglected, since the adsorbed phase has no volume. The above equation is simplified as

$$dU = T\,dS + \sum \mu_i dN_i + \left(\mu_s - \mu_s^*\right)dm_s \qquad (2\text{-}4)$$

The last term in the above relation is the change in surface free energy of solid when contacted with fluid bulk phase. For porous solids, it is solid grand potential Φ

$$\Phi \equiv \mu_s - \mu_s^* \tag{2-5}$$

It cannot be directly measured for porous solids. The following differential equation, called Gibbs adsorption isotherm equation, is utilized to calculate the grand potential. (Talu,2010)

$$d\Phi = -RT \sum n_i d(\ln f_i) \quad (\text{constant T}) \tag{2-6}$$

Where f_i is the fugacity of component i in the bulk gas. n_i is the amount adsorbed based on the solid mass, $n_i = N_i/m_s$.

For an ideal gas phase, Eq. (2-6) reduces to

$$d\Phi = -RT \sum \frac{n_i}{P} dP \quad (\text{constant T}) \tag{2-7}$$

By definition, the grand potential Φ is zero at zero pressure. Thus the grand potential can be calculated from

$$\frac{\Phi}{RT} = -\int_0^P \sum \frac{n_i}{P_i} dP_i \quad (\text{constant T}) \tag{2-8}$$

The integrand $\frac{n_i}{P_i}$ has a finite value at zero pressure, the Henry's constant K_i. It relates to limiting slope of component i isotherm at the origin.[Talu,2010]

$$\lim_{P\to 0}\left(\frac{n_i}{P_i}\right) = \frac{0}{0} = \lim_{P\to 0}\left(\frac{dn_i}{dP_i}\right) = K_i \tag{2-9}$$

Therefore, the integral in Eqn.(2-8) is finite at all pressures.

Isotherm model

The last term $(\mu_s - \mu_s^*)dm_s$ in Eq. (2-4) is the change in surface free energy of solid, when contacted with fluid bulk phase. (Talu, 2010) For adsorption on flat surface, it is often expressed in the form

$$(\mu_s - \mu_s^*)dm_s = \pi \, dA \tag{2-10}$$

Where, π is the spreading pressure, A is the specific surface area. The spreading pressure π, is a crucial intensive variable for adsorption on flat surfaces. From a practical point of view, plenty of isotherm models have been developed for flat surfaces. Most of these models can be converted to equivalent forms for adsorption in microporous substances. Here, the relation between adsorbed phase concentration and the equilibrium vapor pressure is further studied in the following isotherm models from Ruthven's book.[4]

In Ruthven's book, the Gibbs adsorption isotherm is a differential equation and is expressed as

$$a\left(\frac{\partial \pi}{\partial P}\right)_T = \frac{RT}{P} \tag{2-11}$$

a is the molar surface area, also

$$a = \frac{A}{n_i} \tag{2-12}$$

Corresponding to Eq. (2-7) , Eq. (2-11) is converted to

$$A\left(\frac{\partial \pi}{\partial P}\right)_T = \frac{RT}{P} n_i \tag{2-13}$$

n_i is the component i amount adsorbed per unit of solid mass, $n_i = N_i/m_s$. π is the spreading pressure.

The adsorbed phase is characterized by an equation of state in the spreading pressure $A(\pi, T, m_s)$, just as an equation of state V (P, T, N) is used for fluids.

Henry's law

Analogous to ideal gas law, the simplest EOS for the adsorbed phase is expressed as

$$\pi a = RT \tag{2-14}$$

From the Gibbs isotherm Eq. (2-11)

$$\left(\frac{\partial \pi}{\partial P}\right)_T = \frac{RT}{aP} = \frac{\pi}{P} \tag{2-15}$$

Integration at constant temperature gives

$$\pi = \text{constant}(T) * P \tag{2-16}$$

The integration constant is a function of temperature only and it relates to the Henry's Law constant for the adsorbent-adsorbate pair. Combing this equation with the EOS in Eq. (2-11) and Eq. (2-12) gives

$$n_i = \frac{\pi A}{RT} = K \cdot P \tag{2-17}$$

K is the Henry's law constant.

Langmuir (single) Isotherm

The Langmuir model is developed based on three assumptions i) adsorbed layer is a monolayer of finite number of adsorption sites, ii) the surface of solid is uniform and adsorption energy is same for all sites, iii) there is no interacting force among the molecules adsorbed[5].

At higher concentrations, Ruthven et al. postulate the equation of state is formed by

$$\pi(a - \beta) = RT \tag{2-18}$$

in analogy with P (V-b) = N RT,

$$\left(\frac{\partial \pi}{\partial a}\right)_T = -\frac{RT}{(a-\beta)^2} \tag{2-19}$$

Proceeding through the Gibbs isotherm Eq. (2-11), the integration comes to

$$\frac{dP}{P} = -\frac{ada}{(a-\beta)^2} \tag{2-20}$$

Assume $\beta \ll 2a$, which is a reasonable assumption at low concentrations and neglect the term in β^2 in the denominator of Eq. (2-20), above expression integrates to

$$C'(T) * P = \frac{2\beta/A}{1-2\beta/A} = \frac{\Theta}{1-\Theta} = \frac{n_i}{n_i^{\infty}-n_i} \tag{2-21}$$

Θ is the fractional coverage, take $\Theta = 2\beta/A$, and $\Theta = n/n^{\infty}$. As expressed in Eq. (2-21), the total monolayer coverage, $\Theta = 1$, is achieved at infinite equilibrium pressue.

Virial Isotherm

The Virial equation of state gives the best fit at low and medium pressure range as stated by (Zhang and Talu, 1990). The adsorbed phase is considered to obey a general EOS of the Virial form

$$\frac{\pi a}{RT} = 1 + \frac{B'}{a} + \frac{C'}{a^2} + \frac{D'}{a^3} + \cdots \tag{2-22}$$

Take the derivative at constant temperature

$$\left(\frac{\partial \pi}{\partial a}\right)_T = -RT\left(\frac{1}{a^2} + \frac{2B'}{a^3} + \frac{3C'}{a^4} + \frac{4D'}{a^5} + \cdots\right) \tag{2-23}$$

Proceeding through the Gibbs isotherm equation Eq. (2-11) in the same way leads to the Virial isotherm equation

$$\ln P = \text{constant}(T) - \text{Ln } a + \frac{2B'}{a} + \frac{3C'}{2a^2} + \frac{4D'}{3a^3} + \cdots \tag{2-24}$$

Combination with Eq. (2-22), gives an exponential equation

$$P = n_i \cdot \exp\left(\text{constant}(T) - \text{Ln } A + \frac{2B'}{A} n_i + \frac{3C'}{2A^2} n_i^2 + \frac{4D'}{3A^3} n_i^3 + \cdots\right) \tag{2-25}$$

which is reduced to

$$P = n_i \cdot \exp(K + Bn_i + Cn_i^2 + Dn_i^3 + \cdots) \tag{2-26}$$

The Henry's law constant (K) is related to the gas-solid interaction only, while B, C, D…are the Viral coefficients standing for the interactions in the adsorbed phase. Especially, the Henry's law constant plays a significant role in analyzing the adsorbate-adsorbent interactions.

In Eq. (2-26) parameters are inverse functions of T, which can be simplified as follows.

$$K = k_0 + \frac{k_1}{T}; \quad B = b_0 + \frac{b_1}{T}$$

$$C = c_0 + \frac{c_1}{T}; \quad D = d_0 + \frac{d_1}{T} \tag{2-27}$$

In which k_0, k_1, b_0, b_1, etc are temperature-independent Virial coefficients.

Calculation of Henry's Law Constant From Experimental Data

The Henry's Law constant is defined as the slope of the isotherms at the origin. It is a very important thermodynamic property related to the interaction of the molecules with the surface. However, with strongly adsorbed components, it is difficult to determine the Henry's Law constant directly from the limiting slope of the isotherm.

The expression Eq.(2-25) provides the basis of a useful method to evaluate Henry constants from experimental isotherms [Barrer and Davies, 1970].

The Virial equation Eq. (2-26) can be expanded to the following form

$$\ln\left(\frac{P}{n_i}\right) = k_0 + \frac{k_1}{T} + \left(b_0 + \frac{b_1}{T}\right) n_i + \left(c_0 + \frac{c_1}{T}\right) {n_i}^2 + \left(d_0 + \frac{d_1}{T}\right) {n_i}^3 + \cdots \qquad (2\text{-}28)$$

A plot of $\ln(P/n_i)$ versus n_i should be linear at concentration below the Henry's Law limit. The extrapolation of this plot to zero-adsorbed phase concentration provides the simplest way of evaluating the Henry's Law constant. The application of this method has been well recommended by Talu et al [1,4].

Isosteric Heat of Adsorption

The role of temperature in adsorption isotherms is based on the partial differentiation thermodynamic equation:[7]

$$\bar{h} = RT^2 \left[\frac{\partial \ln P}{\partial T}\right]_n \tag{2-29}$$

Or, alternatively

$$q^{IG} = -R \left[\frac{\partial \ln P}{\partial (1/T)}\right]_n \tag{2-30}$$

where $\bar{h}$ is the differential enthalpy of adsorption, a negative quantity because adsorption is exothermic. The absolute value of $\bar{h}$ is called "isosteric heat" which is commonly replaced by symbol q^{IG} to avoid confusion. The superscript (IG) refers to the ideal-gas assumption. In the rigorous real-gas equation, the pressure P is replaced by the fugacity of the gas.

Isosteric heat provides useful information about the nature of the solid surface and the adsorbed phase. The interaction between adsorbate and adsorbent alters the energetics of the system. But it is precisely because of this fact, isosteric heat is path-dependent and is not a good choice to express thermodynamic properties, as stated by Myers [7, 8].

However, isosteric heat indicates the degree of adsorbent heterogeneity and decreases with increasing quantities of adsorbed substances, when the adsorbent surface is heterogeneous. And, it can be calculated from temperature variation of isotherms, without using a calorimetric instrument. It is still an important property to be analyzed in the research and is commonly used in literature [5].

To calculate the isosteric heat, Virial equation of state Eq. (2-24) is considered in this thesis. A good review has been given by Talu. [1] Using pure gas adsorption isotherms at different temperature, the isosteric heat of adsorption of a pure gas is expressed as a polynomial

$$\frac{q^{IG}}{R} = -\left[\frac{\partial \ln P}{\partial(1/T)}\right]_N = -(k_1 + b_1 N + c_1 N^2 + d_1 N^3 + \dots) \qquad (2\text{-}31)$$

Ideal Adsorbed Solution Theory (IAST)

The Ideal Adsorbed Solution Theory (IAST) was first proposed by Myers and Prausnitz in 1965. [9] It quickly became a classic model to predict the multi-component adsorption equilibria, depending on their respective single-component isotherm parameters.

IAST is a predictive model which does not require any mixture data and is independent of the actual model of physical adsorption. [10] It is used to predict the binary mixture adsorption for pairs of gases in silicalite in this study.

IAST is analogous to Raoult's law for vapor-liquid equilibrium, assuming an ideal behavior to represent the relationship between the bulk gas phase and adsorbed phase [4] i.e.:

$$P \cdot y_i = P_i^0(\pi_i) \cdot x_i \text{ (constant T)} \qquad (2\text{-}32)$$

where π_i and x_i are the spreading pressure of component i in the adsorbed phase and molar fraction, respectively. P is the total pressure of the gas mixture. $P_i^0(\pi_i)$ is the standard state pressure of pure component i which yields the same spreading pressure as that of the mixture at same temperature.

Unfortunately, spreading pressure π_i cannot be directly measured for porous solids. According to Myers and Prausnitz research [7], for a pure component system, the integration of the Gibbs adsorption isotherm equation, will give the relationship between spreading pressure π and pure component i isotherm adsorbed n_i^0 in the adsorbed phase.

$$\frac{\pi_i^0 A}{RT} = \int_0^{P_i^0} \frac{n_i^0}{P_i} \cdot d_{P_i} \tag{2-33}$$

For an ideal binary system, Eq. (2-32) and Eq. (2-33) becomes

$$P \cdot y_1 = P_1^0(\pi) \cdot x_1 \tag{2-34}$$

$$P \cdot y_2 = P_2^0(\pi) \cdot x_2 \tag{2-35}$$

$$\frac{\pi_1^0 \mathcal{A}}{RT} = f_1(P_1^0) \tag{2-36}$$

$$\frac{\pi_2^0 \mathcal{A}}{RT} = f_2(P_2^0) \tag{2-37}$$

From pure component isotherm data

$$P_1^0 = f_3(n_1^0) \tag{2-38}$$

$$P_2^0 = f_4(n_2^0) \tag{2-39}$$

For mixing at constant T, the spreading pressure for each component is equal to that for the mixture, therefore

$$\pi_1^0 = \pi_2^0 \tag{2-40}$$

Also,

$$x_1 + x_2 = 1 \tag{2-41}$$

$$y_1 + y_2 = 1 \tag{2-42}$$

Where, x_1 and x_2 represent the molar fraction of either component in the mixture.

In these set of equations, there are eleven unknowns (P, P_1^0, P_2^0, x_1, x_2, y_1, y_2, n_1^0, n_2^0, π_1^0, π_2^0) and nine equations, from Eq.(2-34) to Eq.(2-42). Any two independent variables are specified, all other variables can be calculated at isotherm conditions.

The total amount adsorbed, N (mol/kg) is

$$\frac{1}{N} = \frac{1}{N_1+N_2} = \frac{x_1}{n_1^0} + \frac{x_2}{n_2^0} \ (constant\ T\ and\ \pi) \tag{2-43}$$

So far completes the definition of IAST model.

The selectivity of component 1 over component 2 is defined by

$$S_{1,2} = \frac{x_1/x_2}{y_1/y_2} \tag{2-44}$$

Selectivity is a very sensitive measure of the accuracy of the prediction of the adsorbed-phase composition.

Implementation of Virial model with IAST

With the Virial isotherm equation given in Eq. (2-25).The functionalities for IAST are

$$\frac{\pi_1^0 \mathcal{A}}{RT} = f_1(P_1^0) = K_1 n_1^0 + \frac{B {n_1^0}^2}{2} + \frac{2C {n_1^0}^3}{3} + \frac{3D {n_1^0}^4}{4} \quad (2\text{-}45)$$

$$\frac{\pi_2^0 \mathcal{A}}{RT} = f_2(P_2^0) = K_2 n_2^0 + \frac{B {n_2^0}^2}{2} + \frac{2C {n_2^0}^3}{3} + \frac{3D {n_2^0}^4}{4} \quad (2\text{-}46)$$

$$P_1^0 = f_3(n_1^0) = n_1^0 \exp\left(K_1 + B_1 n_1^0 + C_1 {n_1^0}^2 + D_1 {n_1^0}^3\right) \quad (2\text{-}47)$$

$$P_2^0 = f_4(n_2^0) = n_2^0 \exp\left(K_2 + B_2 n_2^0 + C_2 {n_2^0}^2 + D_2 {n_2^0}^3\right) \quad (2\text{-}48)$$

IAST and Virial equations are used to predict adsorption equilibria for gas mixtures in this work.

CHAPTER III

EXPERIMENT

A. Materials

The silicalite sample as 1/16 inch pellets was purchased from UOP LLC, Illinois, US. The solid sample in this study is in pellet form with an unknown amount of binder. Silicalite crystals have a specific BET surface area of 350 m^2/g [2].

Information about the gases is given in Table I.

TABLE I. Purity of gases used in the study

Gas	Grade	Company
Helium	4.7	VNG, WV, US
Methane	4.0	MATHESON
Ethylene	99.5%	AGA GAS
Propylene	99+%	ACA. INC

Carbon dioxide	Not available	MATHESON

B. Apparatus

The apparatus is designed for measurement of pure and binary component isotherms by volumetric method. The crucial part of the apparatus is the measurement section, which is subdivided into four sections, on the basis of the usage:

1. Inlet section
2. Bypass section
3. Storage section
4. Exit section

A detailed schematic diagram is shown in Figure 1. The inlet (not shown) before valve A1 contains necessary manifold for different gases and outlet (not shown) after valve A11 includes a mechanical vacuum pump and exhaust connections.

The measurement section consists of an adsorption column, a thermocouple inside the column, two storage tanks of different sizes, a flow-rate controller, and two pressure sensors. There are other thermocouples to measure ambient temperature and water bath around the storage tanks. The temperature and pressure readings are collected from indicators connected to the sensors. All of the valves are isolated from the ambient with bellows design. The entire system is 316 stainless steeled.

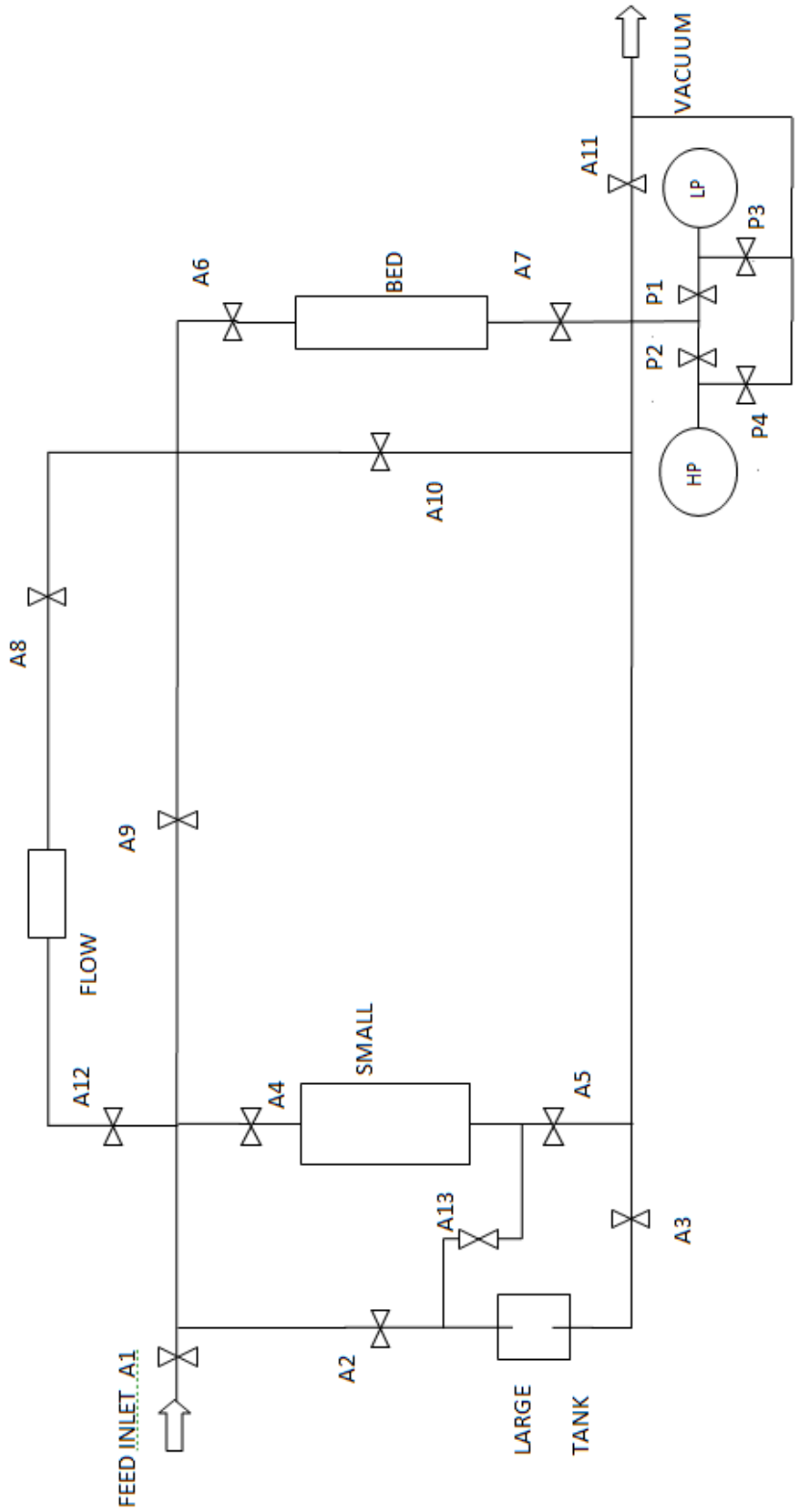

Figure 3.1 Schematic diagram of the experimental system

The adsorption column is made of ½ inch stainless steel tube, situated between the valve A6 and A7. In order to achieve isothermal conditions, the column is kept in a thermostatic waterbath during the measurements, offering a constant temperature surrounding. The water bath is connected to the Fisher Scientific-Isotemp-Heated Bath Circulator, with +- 0.1 C precision.

Activation/ regeneration is achieved by replacing the waterbath with a heating mantle. During activation/regeneration, helium flow through the column is controlled by the flow controller. The activation is performed under vacuum(less than 0.5 psig) with helium flow about 20 cc STP/min. A pre-heating coil before the column is used to heat the helium to activation temperature.

The pressure of the system is monitored by two pressure transducers, which have different ranges. The Low-Pressure transducer, placed between valves P1 and P3, has a 0-15psi range. The High- Pressure transducer, placed between valves P2 and P4, has a 0-100psi range. The pressure transducers are connected to the indicators.

J-type thermocouple is connected to detect the temperature inside the adsorption column. The ambient temperature and the temperature around the storage tanks are also monitored with J-type thermocouples. The specifics, including model number, manufacturer, and the ranges of the instruments are compiled in Table II.

TABLE II Specifics for the instruments

		Model NO.	Manufacturer	Range
Flow controller	Sensor	FMA-133	OMEGA	0-100 SCCM
	Indicator	FMA-2-DPV		
Low_P	Sensor	TJE/713-26	SENSOTEC	0-15 PSIA
	Indicator	60-3147-01		
High_P	Sensor	TJE/713-10	SENSOTEC	0-100 PSIA
	Indicator	60-3147-01		
Temperature	Sensor	J-TYPE	OMEGA	
	Indicator	DP82		
Heater	Jacket	TM518	GLAS*COL	
	Controller	2010	OMEGA	
Water Bath		9005	FISHER SCIENTIFIC	

C. Preliminary experiments

i) Helium expansion/ internal volume determination

In this system, only the volume of the exit section was previously determined by mercury displacement and helium burette techniques. The inside volume of other sections needs to be measured by helium expansion.

Helium expansion is a method to measure the internal volume of a system, by charging helium into the known reference section and expanding it to the target section. The volume of the target section can be calculated from material balances. Adsorption of helium can be neglected under the room temperature. [1] Calculation of volume with

helium expansion technique is similar to the isotherm measurement, the only difference is that the gas amount adsorbed is assumed to be zero. The results of the volume calculation are summarized in Table III.

TABLE III Inside volume of each section in the experimental system

	Section	Enclosed by valves	Volume(cc)	Standard deviation	CV%
Vo-1	Inlet	A1+A2+A4+A9+A12	20.0502	0.2383	1.188
Vo-2	Bypass	A6+A8+A9+A10	9.9614	0.1526	1.532
Vo-3	Exit	A3+A5+A10+A7+A11+P1+P2	14.4835	0.2847	1.966
Vo-4	Pump	-	-	-	-
Vo-5	B-tank	-	-	-	-
Vo-6	Saturator	A2+A3 +A13	162.2194	2.5101	1.547
Vo-7	Low-P	P1+P3	6.5686	0.1334	2.030
Vo-8	High-P	P2+P4	6.4376	0.0974	1.513
Vo-9	Bed (full)	A6+A7	23.4905	0.3666	1.561
Vo-10	S-tank	A4+A5+A13	95.6001	1.4624	1.530
Vo-11	Bed(empty)	A6+A7	25.6431	0.4013	1.565

ii) Experimental protocol

The procedure, basically, consists of activation, gas charge and equilibration procedures. Prior to each adsorption experiment, the sample was activated at 310C under vacuum with helium flush flow overnight ensuring a negligible residual amount adsorbed. After

activation, charge and equilibration steps are repeated several times to collect isotherm data.

ACTIVATION AND COOL-DOWN

1. BRING TO STAND BY CONDITION
2. Open Valves;
   - ·open exit valve A11, if the system is above atmospheric pressure
   - ·open all valves except inlet valve A1
3. Vacuum system;
   - ·close air bleed valve, start the mechanical vacuum pump
   - ·wait until pressure indicators show lowest vacuum
   - ·close all valves except P1 and P2
4. Start helium flow;
   - ·switch inlet gas to helium
   - ·open helium cylinder valve and regulator exit valve, set pressure above 10psig
   - ·open A1, A12, A8, A10 and A11, flow indicator should show helium flow-rate
   - ·slowly open A6 and A7, close A10 to direct helium flow through the column
5. Start heating;
   - ·set up the heating mantle, confirm the adsorption column and furnace wall are not in contact, confirm the control thermocouple is placed in the mantle
   - ·start Heat-controller
6. Leave the system for activation over-night;

7. Stop the flow;

   ·record the system condition

   ·close A1, A12, A8 and A6

   ·close helium cylinder and regulator valves

8. Full vacuum;

   ·wait for full vacuum, close A11

   ·record system condition, close A7 to isolate the column

9. Cool down

   ·open the air bleed valve and stop the vacuum pump

   ·set T-controller to under zero

   ·unplug the heating mantle and remove it

   ·wait until the sample TC reads desired ambient temperature

ISOTHERM EXPERIMENTS

1. First step after activation;(column should be isolated, and cooled)

   ·place water bath around the column, set up water circulation, adjust controller to desired isotherm temperature

   ·switch inlet to desired gas

   ·open gas cylinder valve, set regulator pressure

   ·open A1, A9, A10 and A11 to let some gas go through A11 directly to vacuum, then close A10

   ·after full vacuum, close A11

·flush with gas, open A10 slowly, fill the exit part and small tank to 2-5 psi, close A10, open A11 slowly, vacuum full, close A11, repeat one more time

2. Charge pressure step if it is lower than 15psi(otherwise, skip to 3 below, if P charge> 15 psi)

   ·fill gas to desired pressure by opening A10 slowly

   ·close A10

   ·set chart-recorder, and record charge pressure, T-column, T-ambient and T-jacket

3. Charge pressure step if it is higher than 15 psia but lower than 100 psia

   ·isolate low-P regulator, close P 1

   ·fill gas to desired pressure by opening A10 slowly

   ·close A10

   ·set chart-recorder, and record charge pressure, T-column, T-ambient and T-jacket

4. Wait for equilibrium step

   ·open A7 slowly and completely (keep A6 closed)

   ·wait for the equilibrium until the pressure remains unchanged in 1 hour

   ·record equilibrium pressure, T-column, T-ambient and T-jacket

·close A7

5. Repeat step 2(or 3) and 4, varying the charge pressure as desired

6. Go to stand-by condition

·close A1, open all valves except A11

·if the system is above atmospheric pressure open A11 to reduce pressure

·close all valves except P1 and P2

·stop water circulator, remove the water bath

· open air bleed valve and turn off the vacuum pump if operating

· leave the system

e). Calculation Procedure

Using the material balance, the amount adsorbed at each step is

$$n_{diff} = n_{in} - n_f$$

In which,

$$n_{in} = \left[\frac{V_{column}}{v_{column}(T_{column,} P_{eq}^{i-1})}\right]_{charge} + \left[\frac{V_{charge}}{v_{charge}(T_{charge,} P_{charge})}\right]_{charge}$$

n_{in} is the initial number of moles present at each charge step. V_{column} is the volume of the column. V_{charge} is the charge volume in the system. $v_{column}\ and\ v_{charge}$ are the molar volumes of the gas, at the respective T, P conditions. Virial Equation of State is used with second Virial constants taken from DIPPR database for the molar volumes.

$$n_f = \left[\frac{V_{column}}{v_{column}(T_{column,}P_{eq}^{i})}\right]_{eq} + \left[\frac{V_{charge}}{v_{charge}(T_{charge}P_{eq}^{i})}\right]_{eq}$$

n_f is the final number of moles present at each equilibrium step.

Thus, amount adsorbed per mass adsorbent at each step is

$$\Delta n_i = {}^{n_{diff}}/_{weight\ of\ adsorbent}$$

The isotherm data is collected by changing the conditions. The amount adsorbed is calculated from

$$n_i = \sum \Delta n_i$$

Where it is zero after activation by definition. The relation between n_i and P_{eq}^{i} is the isotherm at the respective column temperature.

CHAPTER IV

RESULTS AND DISCUSSION

In this section the analysis of all pure component experiments are presented first, followed by a section where the experimental results are compared with isotherm models.

A. Pure Component Adsorption Isotherms of Methane, Ethylene, Propylene and Carbon Dioxide in Silicalite

Pure component adsorption isotherms were obtained volumetrically at three different temperatures, as 10C, 35C and 65C. The pure component excess adsorption isotherms of methane, ethylene, propylene and carbon dioxide in silicalite are presented in Figures 4.1 through 4.4.

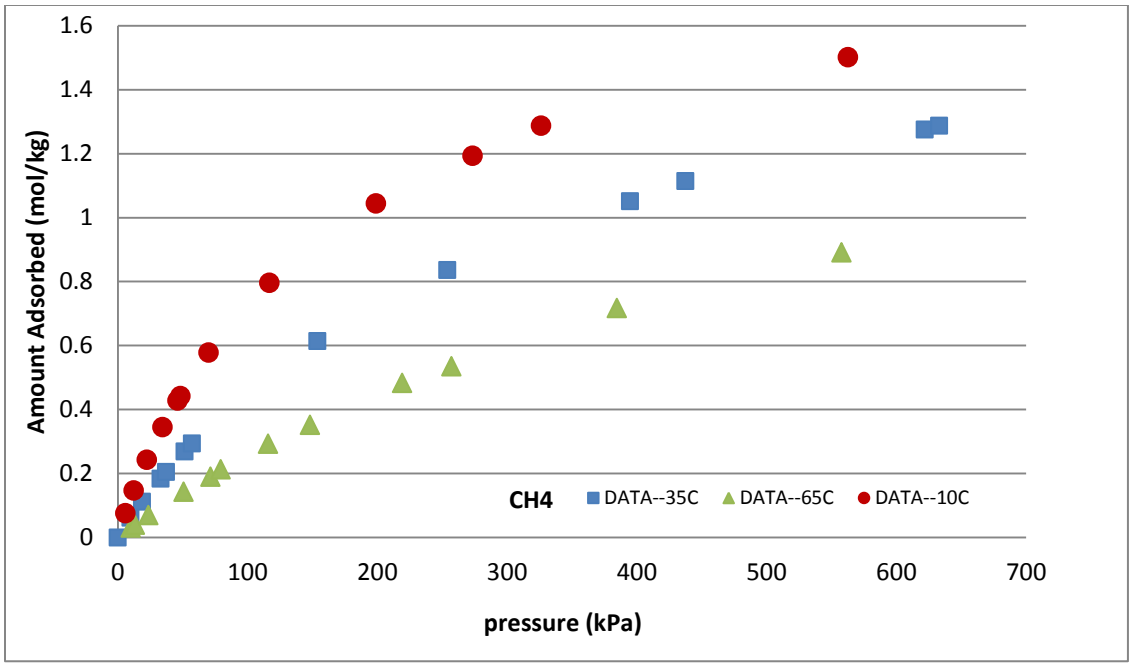

Figure 4.1 Adsorption Isotherm of methane in silicalite

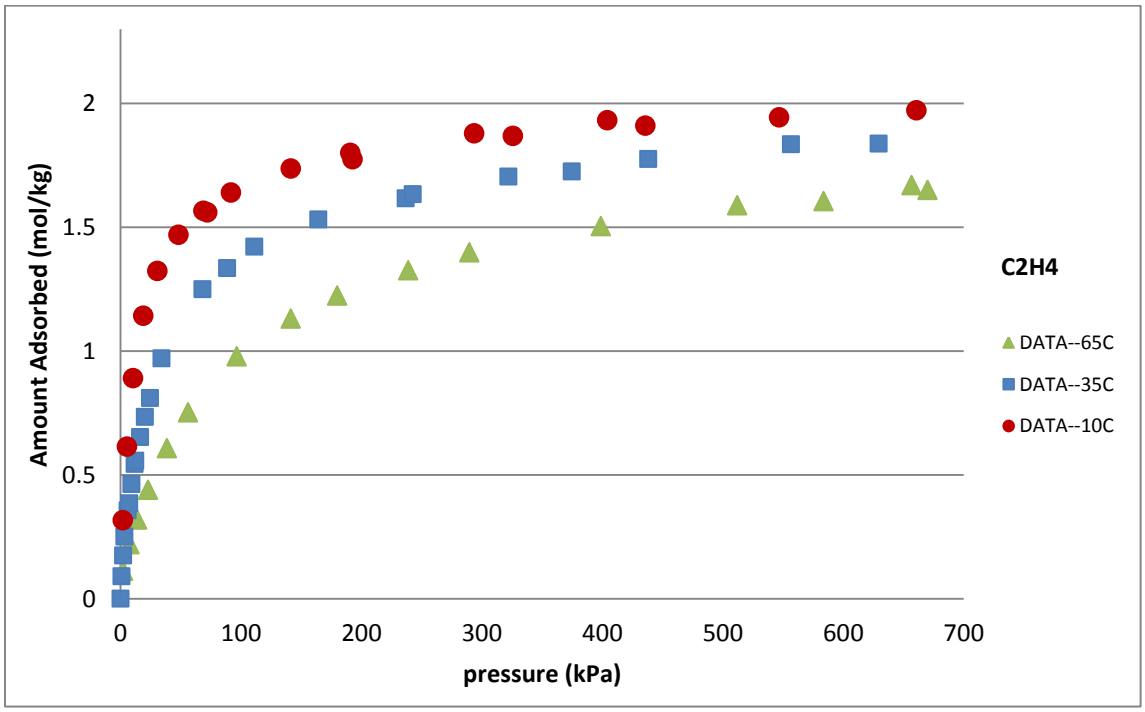

Figure 4.2 Adsorption Isotherms of ethylene in silicalite

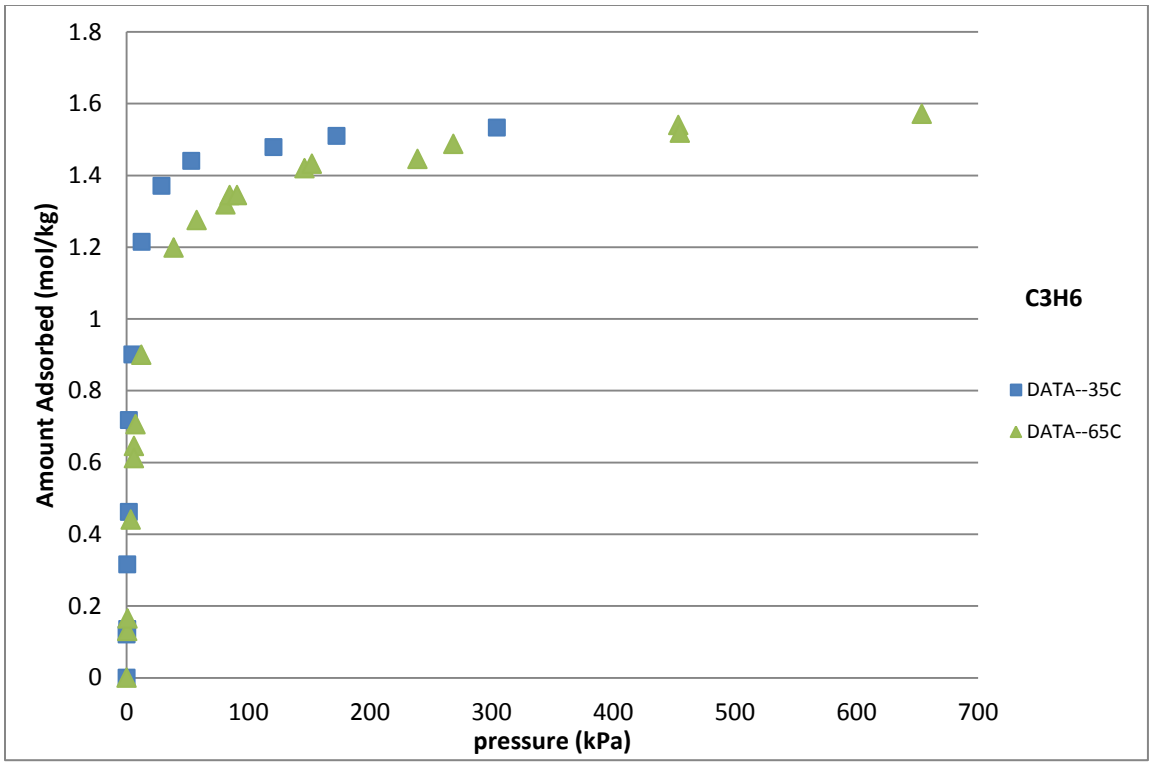

Figure 4.3 Adsorption Isotherms of propylene in silicalite

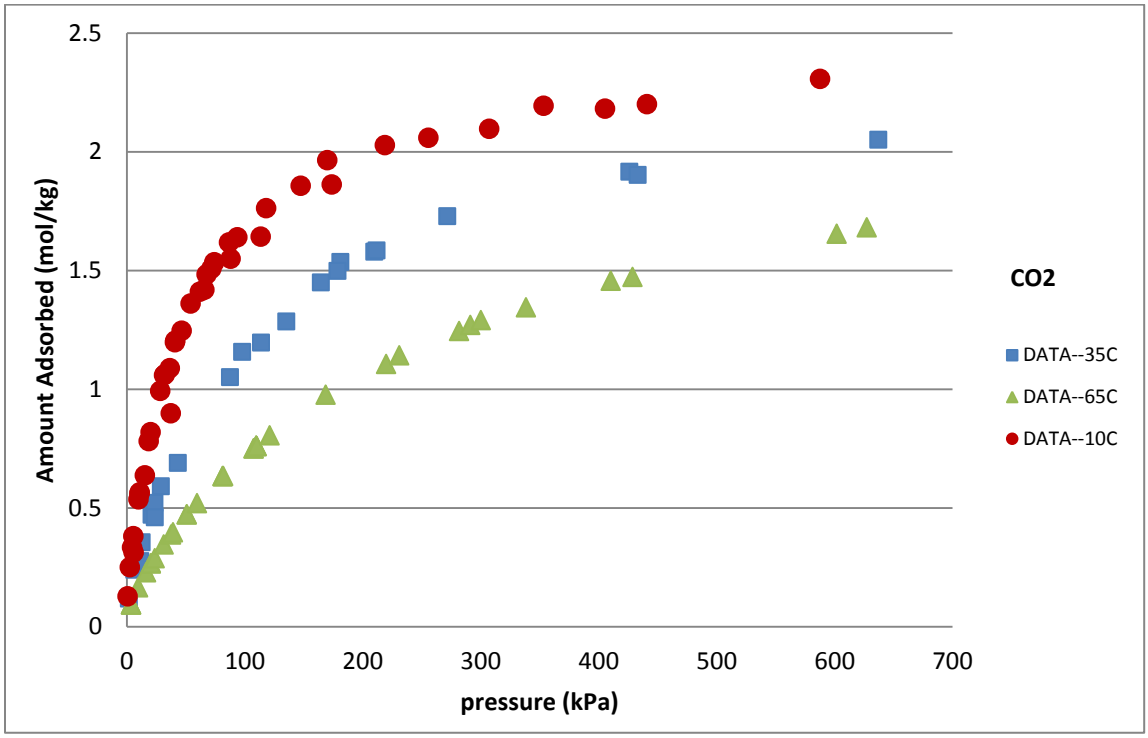

Figure 4.4 Adsorption Isotherms of carbon dioxide in silicalite

Any gas adsorption isotherm in a micro-porous solid has two important characteristics:

1) The saturation capacity as indicated by the plateau level at high pressures

2) The Henry's constant as indicated by the slope at origin

The saturation capacity is determined by molecular size and micro-pore space available in the solid. For the same solid, the saturation capacity decrease as molecular size increases. For the four gases studied so far, the saturation capacities are in the order CO2>CH4>C2H4>C3H6

This order is deduced, although the CH4 isotherms did not reach high enough plateau pressure levels.

Another way to analyze the experimental data is from the slope at origin of the isotherm, which is the Henry's constant. Henry's constant of a gas is determined by the affinity of the solid or the strength of attractive forces between the solid and gas molecules [2]. According to the comparisons of the slopes under same temperature for four gases, the order of Henry's constant is C3H6>C2H4>CO2>CH4.

B. Pure Component Isotherm Regressions

The purpose of regression of the pure component data for a model was to express the data in an analytical form to facilitate binary calculations. The pure component data were fitted with two models:

i) Virial model

ii) Langmuir model

Virial Regressions

Regressions were performed on the pure component data to determine the number of Virial coefficients. A statistic software, Sigmastat, was used. Isotherm data at all temperatures were used in a single multiple linear regression with model equations given in Eqn. (2-28). The best fitting model was chosen by the F-statistics of the overall regression by forward stepwise technique with a significance level of 0.05. The significance levels based as T-statistics is also given in the table IV. Since $T_{value} < T_{0.01}$, the null hypothesis that parameter equal to 0 will be rejected.

The estimated Virial coefficients obtained from the data analysis for the adsorption of methane, ethylene, propylene and carbon dioxide in silicalite are presented in Table IV along with standard deviation of parameters.

TABLE IV. Virial Coefficients for the adsorption isotherms

	Methane			Ethylene		
	Value	Std.dev	T-statistics	Value	Std.dev	T-statistics
k0	13.41	0.0474	0.0035	12.771	-	-

k1	-2584.67	15.201	-0.0059	-3403.24	-0.635	0.0002
b0	0.212	0.0993	0.4684	3.82	1.927	0.5045
b1	236.72	27.938	0.1180	-	-	
c0	-0.457	0.0699	-0.1529	-1.154	-1.275	1.1049
c1	-	-		-596.623	-2.261	0.0038
d0	0.32	0.0316	0.0988	-	-	
d1	-	-		368.99	2.735	0.0074
	Propylene			Carbon Dioxide		
	Value	Std.dev	T-statistics	Value	Std.dev	T-statistics
k0	14.86	-	-	14.411	-	-
k1	-4711.13	-0.392	0.0009	-3699.9	--0.995	-0.0003
b0	-	-	-	1.627	1.105	0.6792
b1	1671.751	1.503	0.0008	719.172	1.705	0.0024
c0	-	-	-	-2.902	-4.55	1.5679
c1	-2293.08	-3.71	0.0016	-	-	-
d0	-	-	-	1.415	4.729	3.3420
d1	1237.059	3.193	0.0025	-167.952	-1.954	0.0116

The Experimental data points and the Regressions of Virial equation (dashed lines) are shown in Figure 4.5-4.8. Because the experimental data are measured using the volumetric method, the experimental error in the calculated amount adsorbed, n_I, accumulates such that the last measured point is the least accurate.

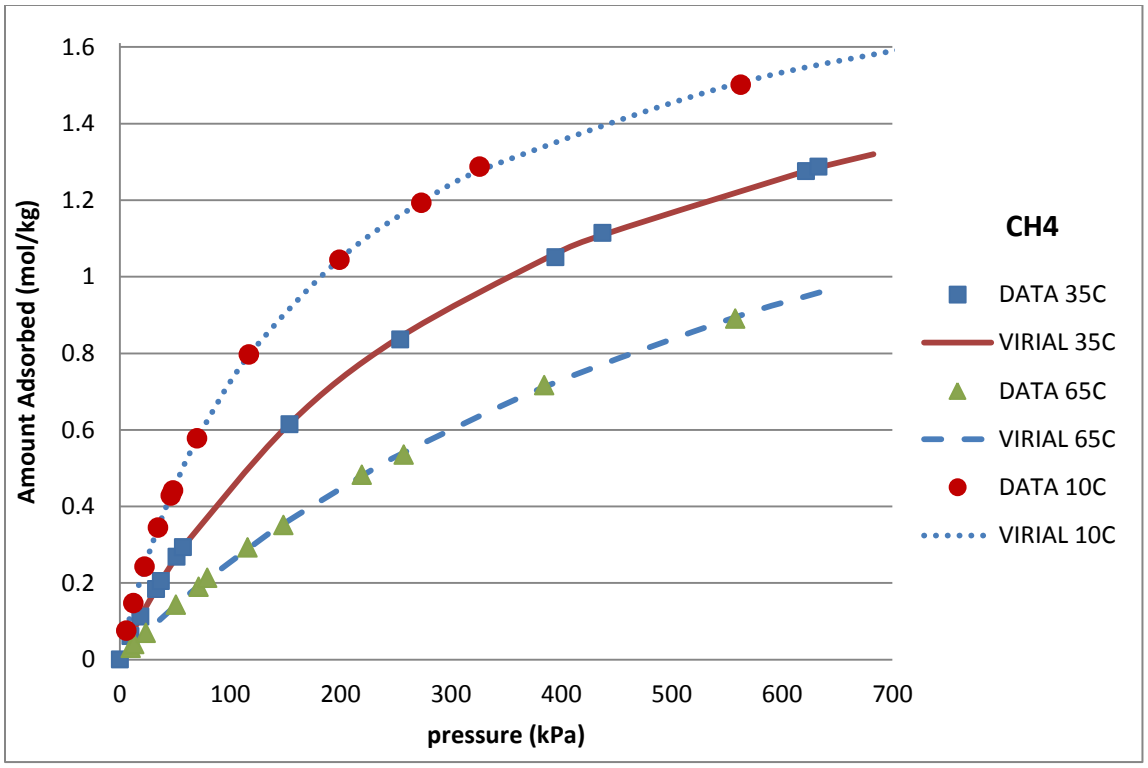

Figure 4.5 Virial Regressions and experimental data for Pure Methane

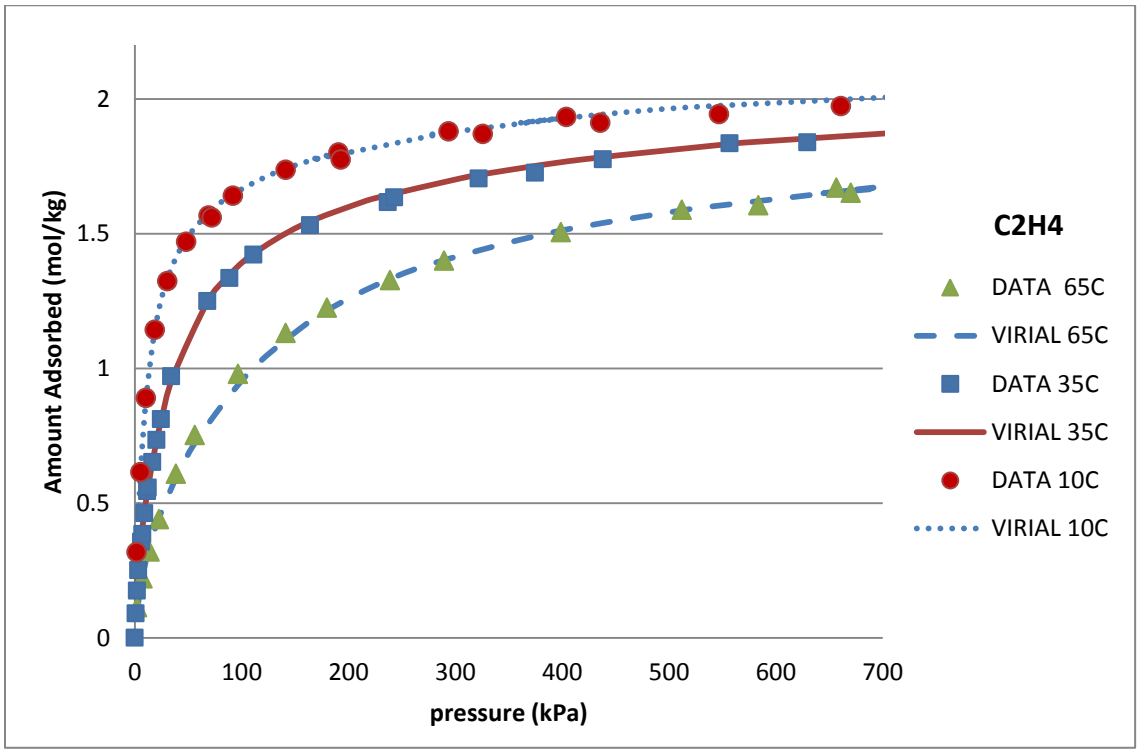

Figure 4.6 Virial Regressions and experimental data for Pure Ethylene

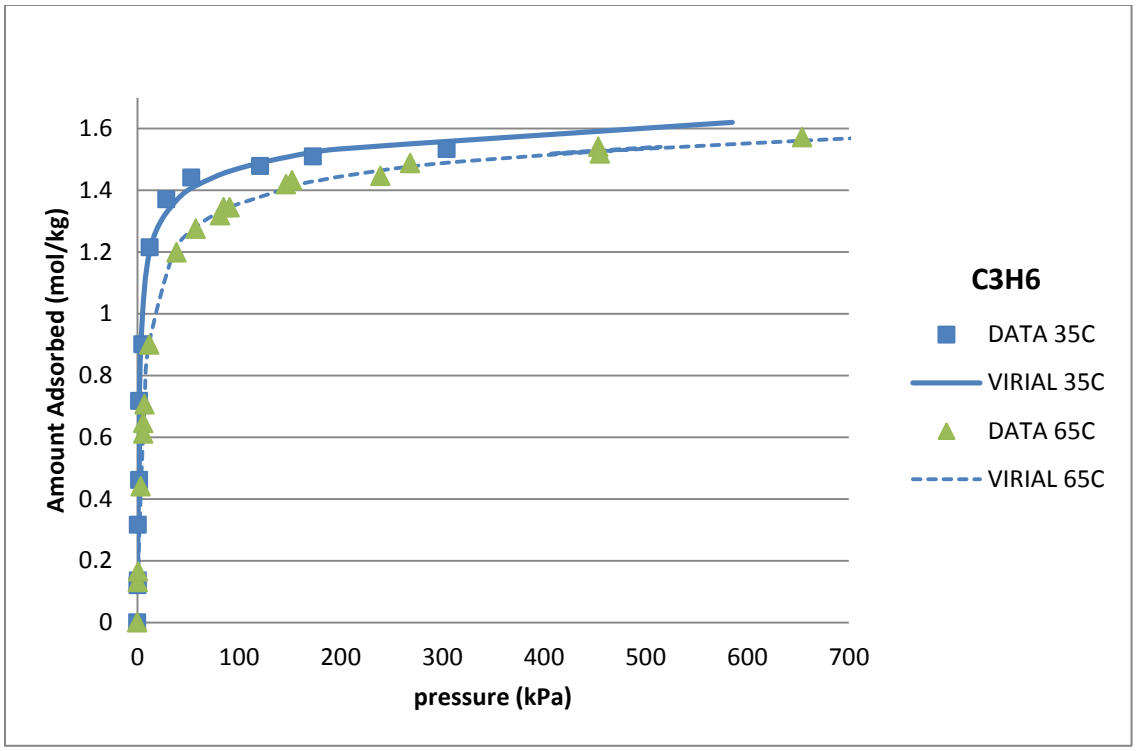

Figure 4.7 Virial Regressions and experimental data for Pure Propylene

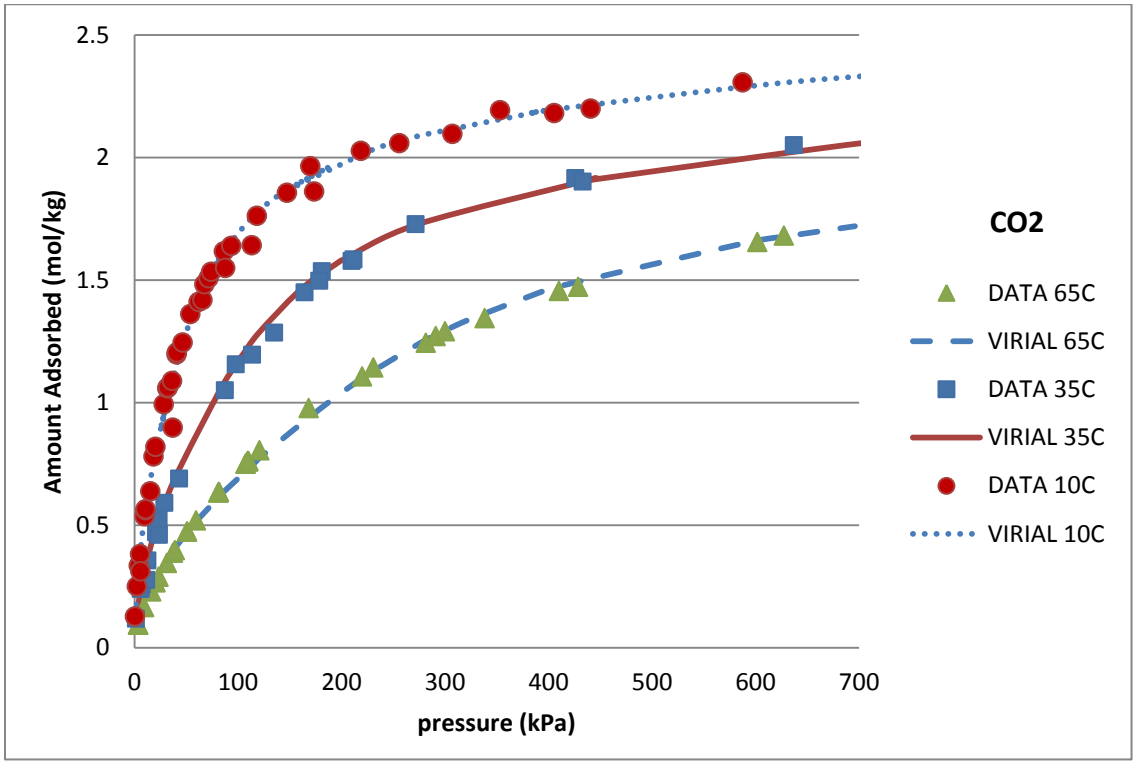

Figure 4.8 Virial Regressions and experimental data for Pure Carbon Dioxide

From these figures 4.5 through 4.8 and the statistics given in Table 7 it can be seen that the isotherm data are well correlated by Virial Model.

Silicalite powder was used as adsorbent in literature [3]. Silicalite pallets with about 20% binder are used in this study.

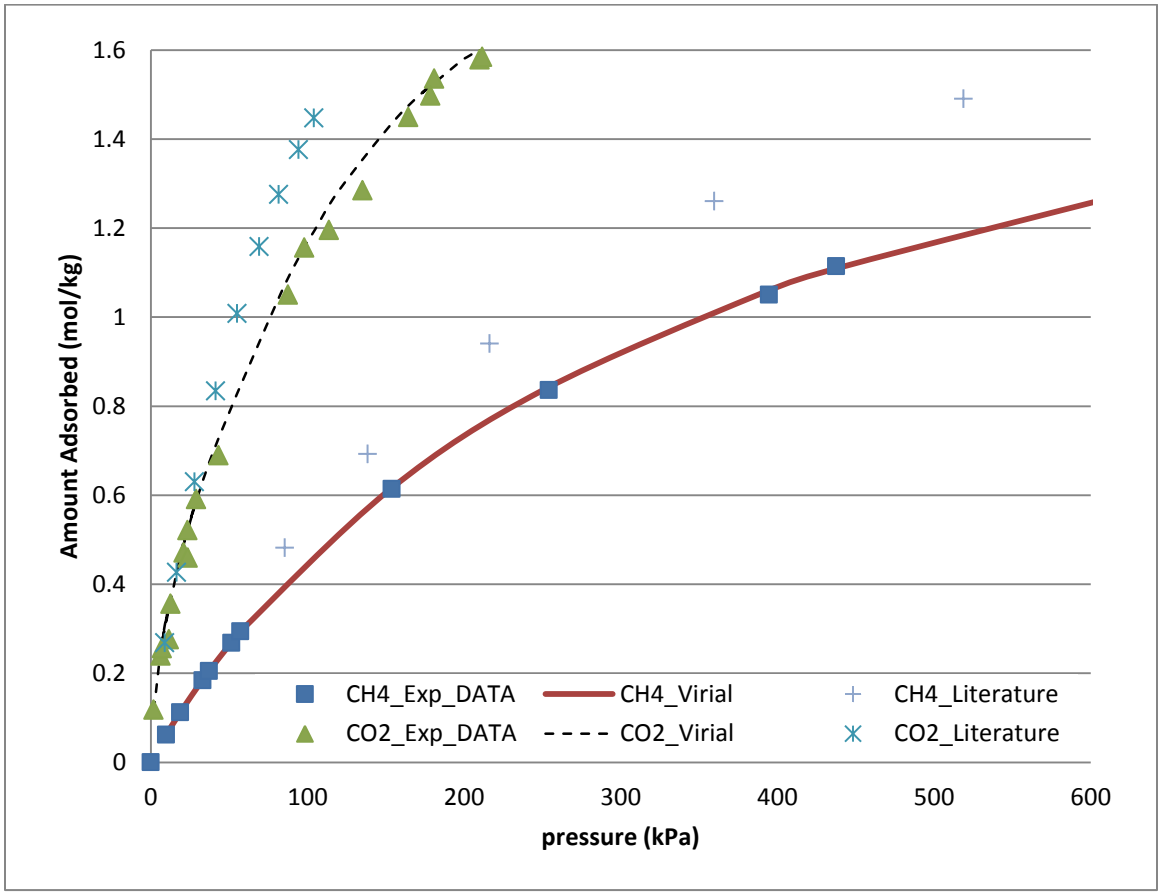

Figure 4.9 Comparison between experimental data and literature data under 35C

Langmuir Regressions

Linear regressions are also used to estimate the parameters of Langmuir isotherm model. The model is first linearized followed by simple linear regression. Table V presents a common linearization of the Langmuir isotherm used in this study and the regressed parameter values by the least-squares method.

TABLE V. Isotherm parameters for the adsorption isotherms

Linear Regression	Coefficients	Adsorbent			
		Methane	Ethylene	Propylene	Carbon Dioxide
$\frac{P}{n} = \frac{1}{bn^{\infty}}P + \frac{1}{n^{\infty}}$	**T = 10C**				
	$1/n^{\infty}$	81.689	7.751	-	15.965
	b	0.0065	0.0648	-	0.0262
	R^2	0.9984	0.9992	-	0.9962
	T = 35 C				
	$1/n^{\infty}$	162.31	14.978	2.1846	35.547
	b	0.0033	0.0353	0.2964	0.0125
	R^2	0.9984	0.9976	0.9998	0.9889
	T = 65 C				
	$1/n^{\infty}$	330.6	34.801	7.5975	71.103
	b	0.0030	0.0162	0.0836	0.0073
	R^2	0.9945	0.9922	0.9994	0.9664
Units: P in kPa; n and n^{∞} in mol/kg;					

Once Langmuir parameters are estimated, the assessment of goodness-of-fit is discussed by the R-square statistics. The table also contains R-square values to assess

the goodness–of-fit. In general, R-square values are very high with lowest being 0.9664. This would normally be an excellent representation of data with the model in the regression domain as P/n VS. P. Figure 4.10 to 4.13 graphically display the regressions. Examination indicates that Langmuir model captures most of the essence of data but deviates at low pressures (in the Henry's Law region). This is particularly apparent in Figure 4.12 for CO2. The Henry's Law region is extremely important in adsorption since it denotes the basic affinity of the solid for the gas species.

The comparison of the Experimental data with correlation results from Langmuir model for pure methane, ethylene, propylene and carbon dioxide are illustrated in Figure 4.10 through 4.13 in the linearized domain.

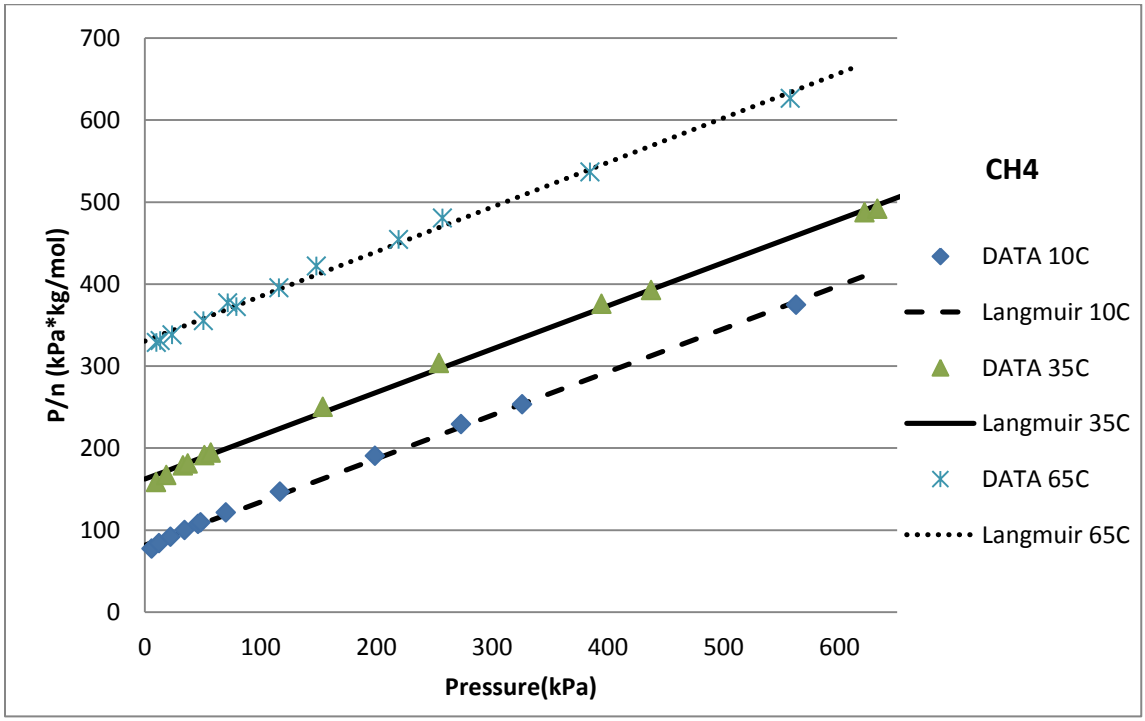

Figure 4.10 Langmuir Regressions and Experimental Data for Pure Methane

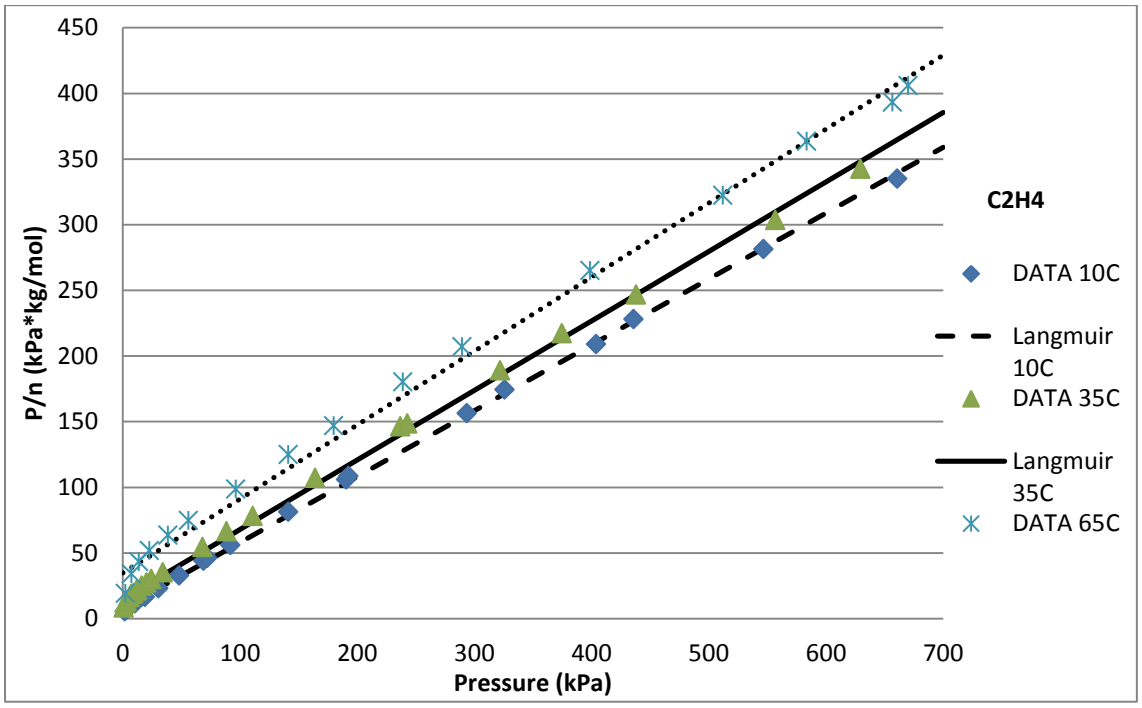

Figure 4.11 Langmuir Regressions and Experimental Data for Pure Ethylene

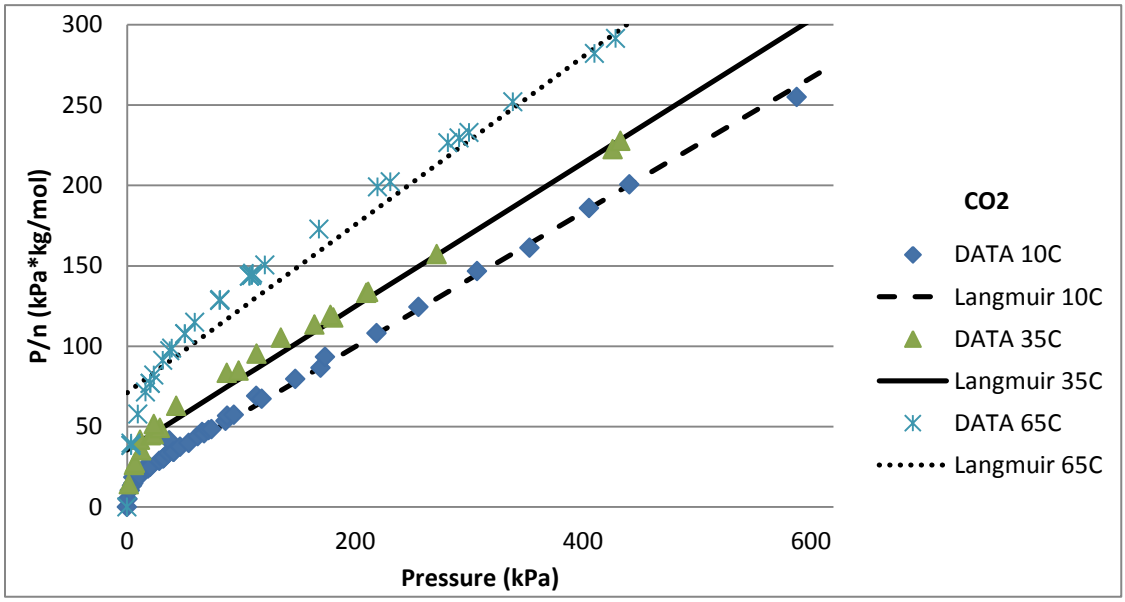

Figure 4.12 Langmuir Regressions and Experimental Data for Pure Carbon Dioxide

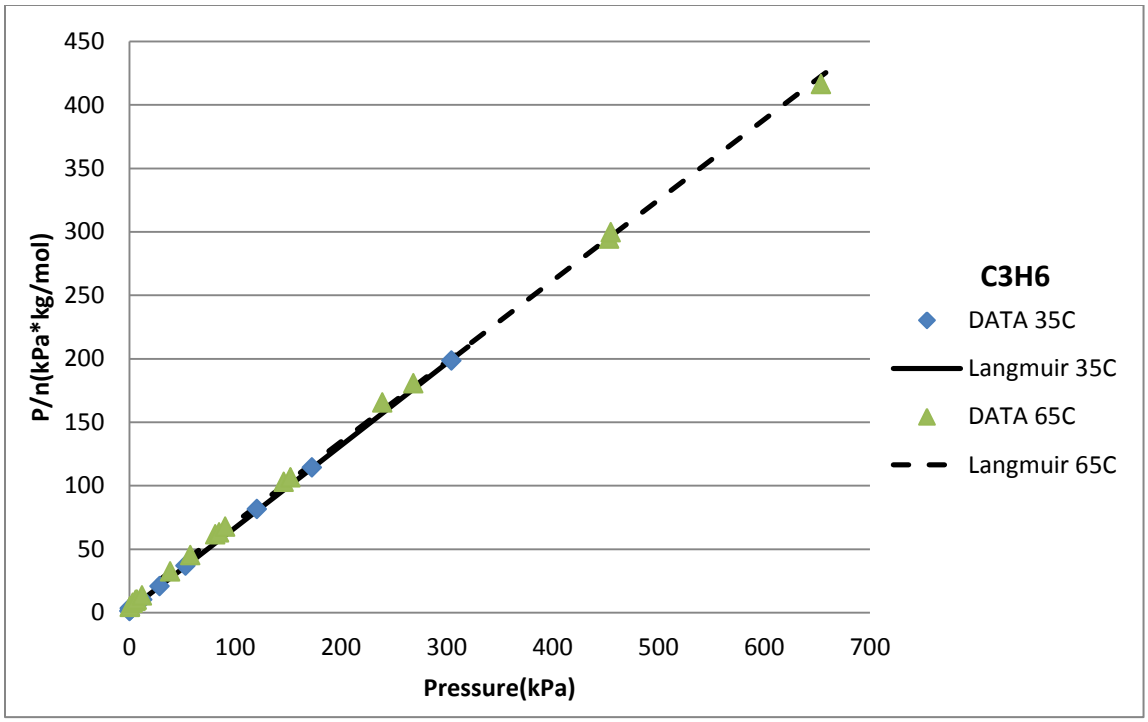

Figure 4.13 Langmuir Regressions and Experimental Data for Pure Propylene

C. Comparison of the models

The Virial and Langmuir models have different structures and contain different number of parameters. In general, accuracy of a model to reproduce data increases with increasing number of parameters. Therefore, comparison of different models in this section is not a straightforward task.

One method that is commonly employed is to calculate sum-of-square errors (SSE) for the models. SSE is defined as,

$$SSE = \sum_{i=1}^{all\ points} \left(P_i^{exp} - P_i^{model}\right)^2 \quad (7\text{-}1)$$

The sum-of–squares error (SSE) is a function of residues, the differences between the experimental data and predicted values (pressure in this case) given by mathematical models. The smaller SSE, the better the approximating function Regressions the data. Table VI below lists the SSE for the data set in this study.

TABLE VI. Comparison of Sum of Square Error for two different regression models

Sum of Square Error				
	CO2		C2H4	
	Langmuir	Virial	Langmuir	Virial
10C	216249.07	8019.21	818756.00	36366.65
35C	48757.71	3402.29	347058.64	6699.16
65C	201864.75	1620.69	145185.44	3149.01
	CH4		C3H6	
	Langmuir	Virial	Langmuir	Virial

10C	967.24	146.99	-	-
35C	784.28	94.49	33986.91	12666.68
65C	278.75	56.97	15806921.87	13911.81

Examination of Table VI indicates that the Virial isotherm represents the dataset much more accurately in this study. In addition, it provides T-independent parameter values directly which is more convenient to use in binary predictions. Therefore, the Virial isotherm equation with parameters given in Table IV is used in the mixture predictions with the IAST model.

D. Virial domain

The isotherm plots Figure 4.1 through 4.8 do not reveal any detail in the low pressure to assess quality of data. However, Henry's constant is a very important thermodynamic property related to the interaction of the molecules with the surface [2]. Therefore Henry's constant values carry a significant weight in determining binary phase diagrams. Very accurate data at low pressure are necessary to accurately determine Henry's constants.

A 'Virial domain' definition reported in literatures [1,4,12] reveals information about the Henry's Law constant and the quality of data at low pressure, by plotting the isotherm data as ln(P/n) versus n. The intercept at zero amount adsorbed is related to Henry's Law constant. The Virial domain plots Figure 4.14 through 4.17 are used to scrutinize data.

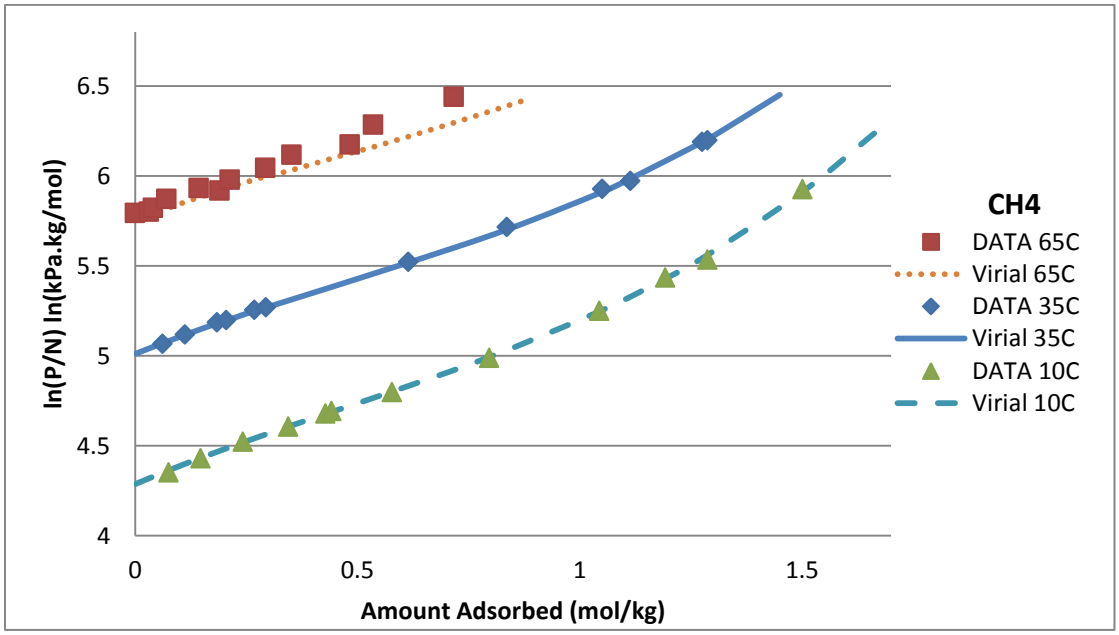

Figure 4.14 Virial plot of ln(P/n) versus n for methane in silicalite.

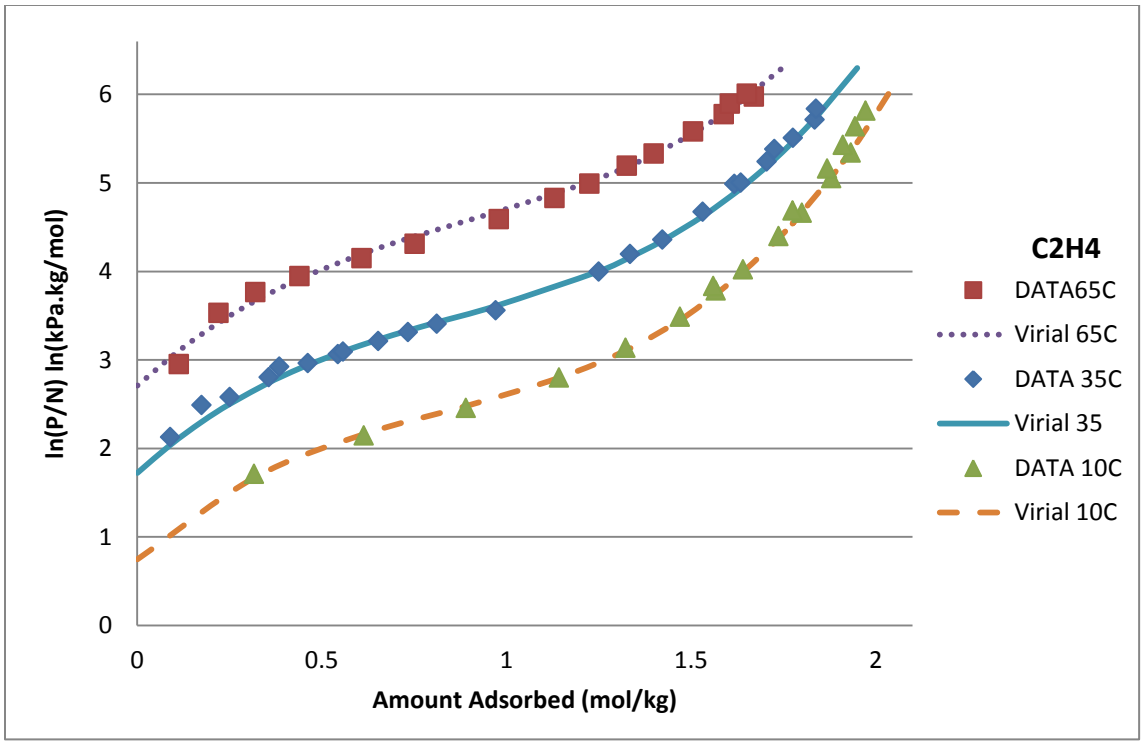

Figure 4.15 Virial plot of ln(P/n) versus n for ethylene in silicalite.

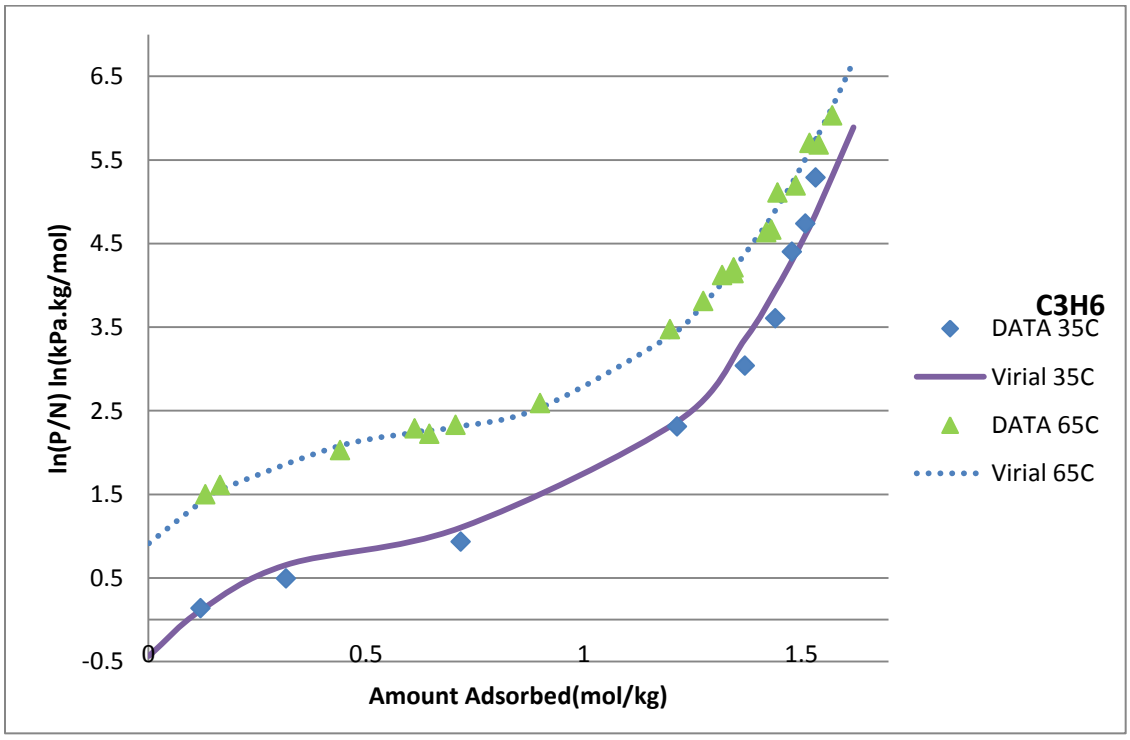

Figure 4.16 Virial plot of ln(P/n) versus n for propylene in silicalite.

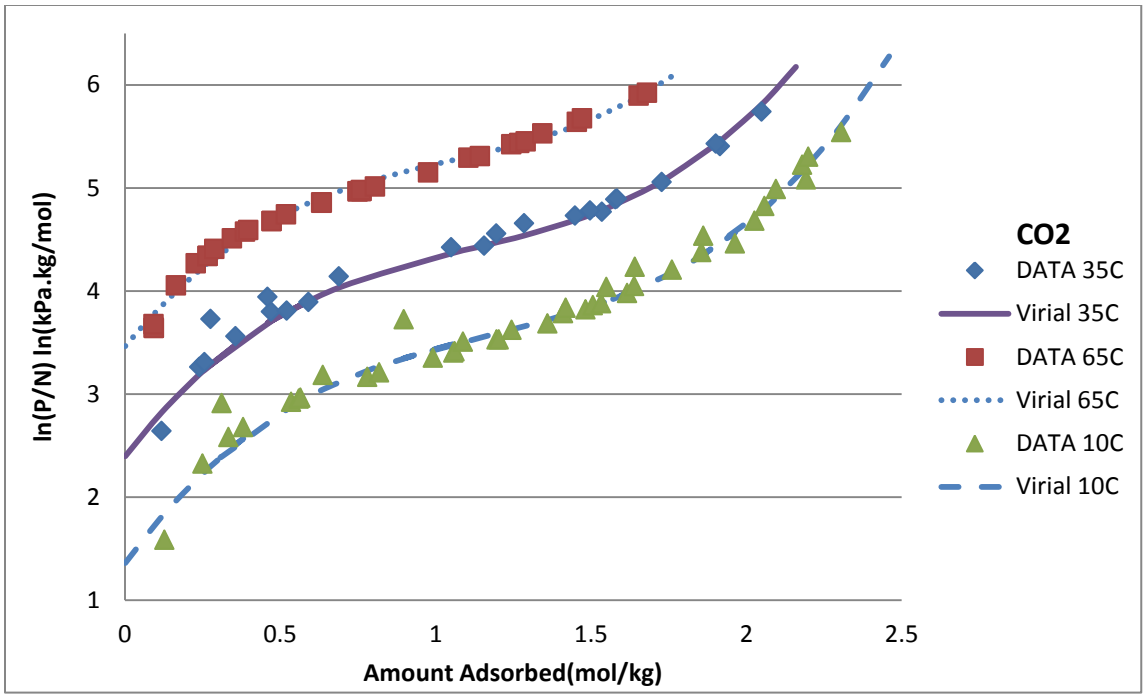

Figure 4.17 Virial plot of ln(P/n) versus n for carbon dioxide in silicalite.

As shown in Figure 4.14 through 4.17, the experimental data presented here has excellent accuracy for most with some scatter for C3H6 and CO2 at lower temperatures. Furthermore, these figures also show the Virial equation greatly following the data at low pressure. The Virial equation is found to be a reliable way to calculate the Henry's law constants with good accuracy.

E. Prediction of Binary Adsorption Equilibrium Using IAST-Virial model

This section discusses in detail the predictions made by IAST-Virial model. IAST-Virial model is the combination of IAST theory and the Virial isotherm equation. The predictions of the binary adsorption by the IAST-Virial model are quite straightforward and completely based on the obtained temperature independent parameters of the pure-component adsorption models as shown by Tables IV. Temperature-dependent coefficients used in the binary adsorption predictions are given in Table VII.

TABLE VII. Coefficients used in binary adsorption predictions

Adsorbate	Methane	Ethylene	Propylene	Carbon Dioxide
T = 10 C=283.15K				
K	4.2817	0.7518	-1.7783	1.3441
B	1.0480	3.8200	5.9041	4.1669
C	-0.4570	-3.2611	-8.0985	-2.9020
D	0.3200	1.3032	4.3689	0.8218
T = 35 C=308.15K				
K	5.0223	1.7269	-0.4284	2.4042
B	0.9802	3.8200	5.4251	3.9608
C	-0.4570	-3.0901	-7.4415	-2.9020
D	0.3200	1.1974	4.0145	0.8700
T = 65C=338.15K				
K	5.7664	2.7067	0.9279	3.4694
B	0.9120	3.8200	4.9438	3.7538
C	-0.4570	-2.9184	-6.7813	-2.9020
D	0.3200	1.0912	3.6583	0.9183
*Units; Pressure in kPa, Amount adsorbed in mol/kg, Temperature in K.				

MATLAB is used in this study to calculate the total amount adsorbed in different binary systems and the computer code is given in Appendix A. In order to better analyze binary

mixture predictions, the data are represented in 3-D and 2-D plots, in three variations: pressure, gas composition and temperature. For the first two variations, isothermal condition at 35 °C is selected as the base common temperature for each predicted binary system.

a) 3-D plots for total amount adsorbed in binary adsorption prediction

The effect of total pressure and gas composition in total amount adsorbed are presented in 3-D graphs from Figure 4.18 to 4.23 to provide a vivid description of the predicted total amount adsorbed in various conditions. E.g. Figure 4.18 is the total amount adsorbed for CO2/C2H4 mixture in silicalite.

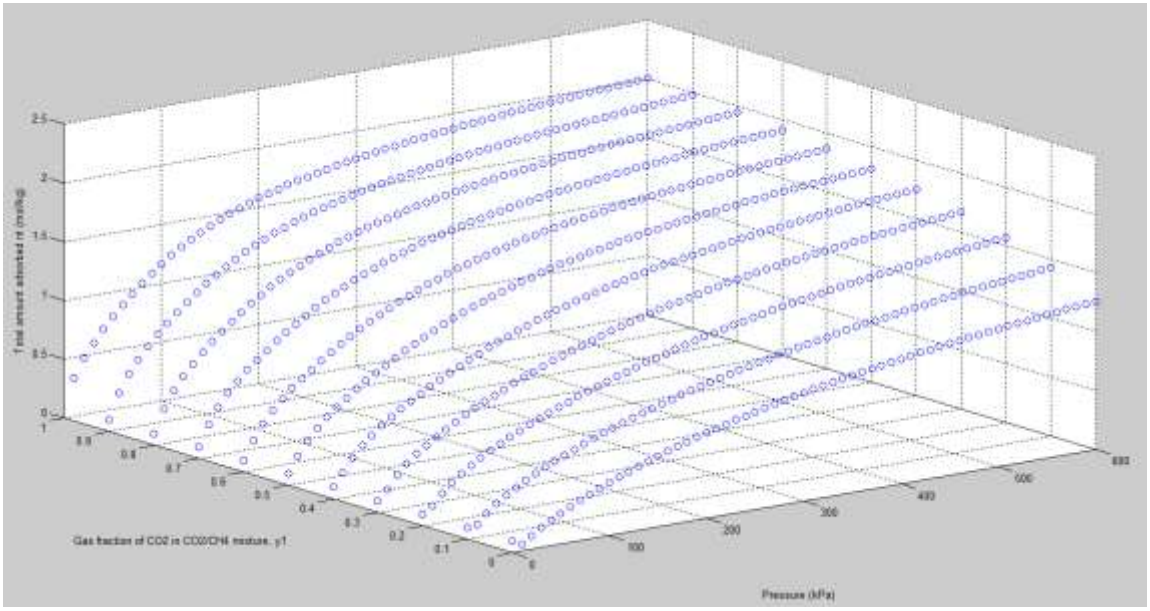

Figure 4.18 Total amount adsorbed for CO2/CH4 mixture in fraction of pressure and gas composition

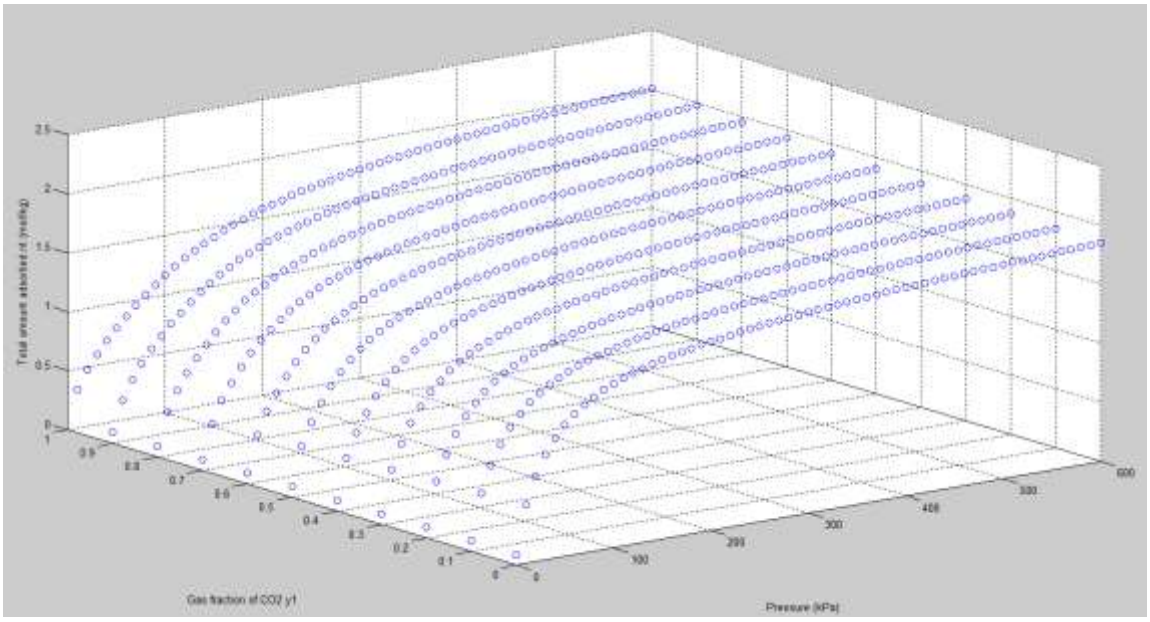

Figure 4.19 Total amount adsorbed for CO2/C2H4 mixture in fraction of pressure and gas composition

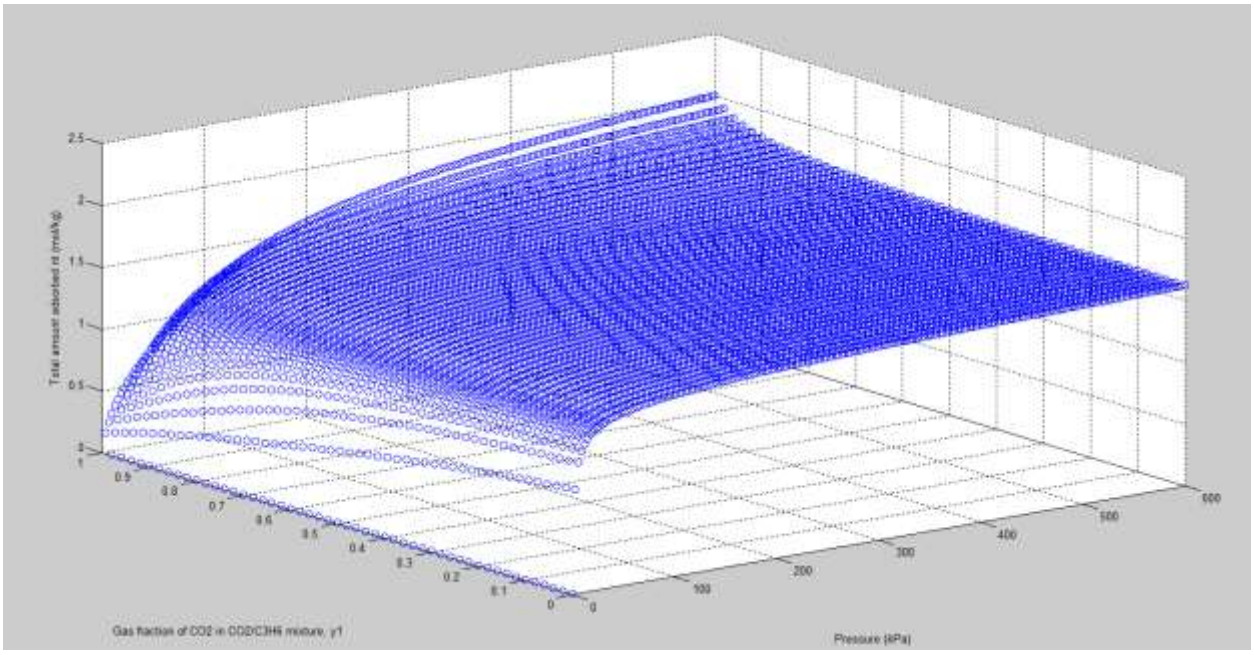

Figure 4.20 Total amount adsorbed for CO2/C3H6 mixture in fraction of pressure and gas composition

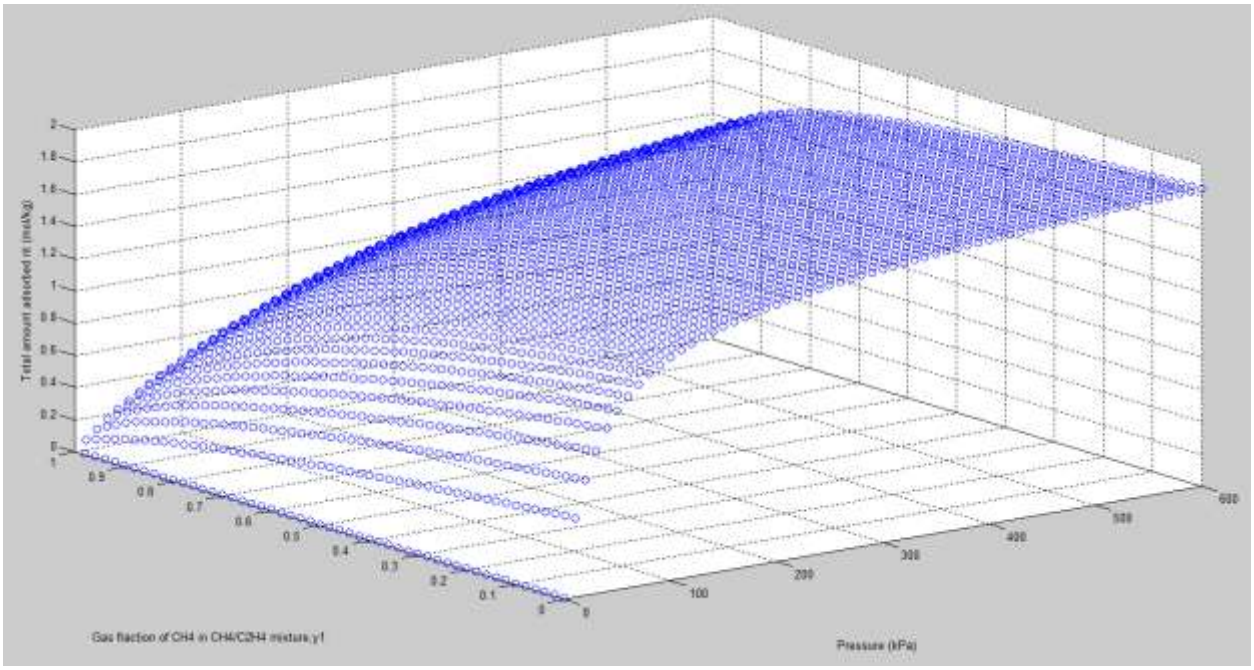

Figure 4.21 Total amount adsorbed for CH4/C2H4 mixture in fraction of pressure and gas composition

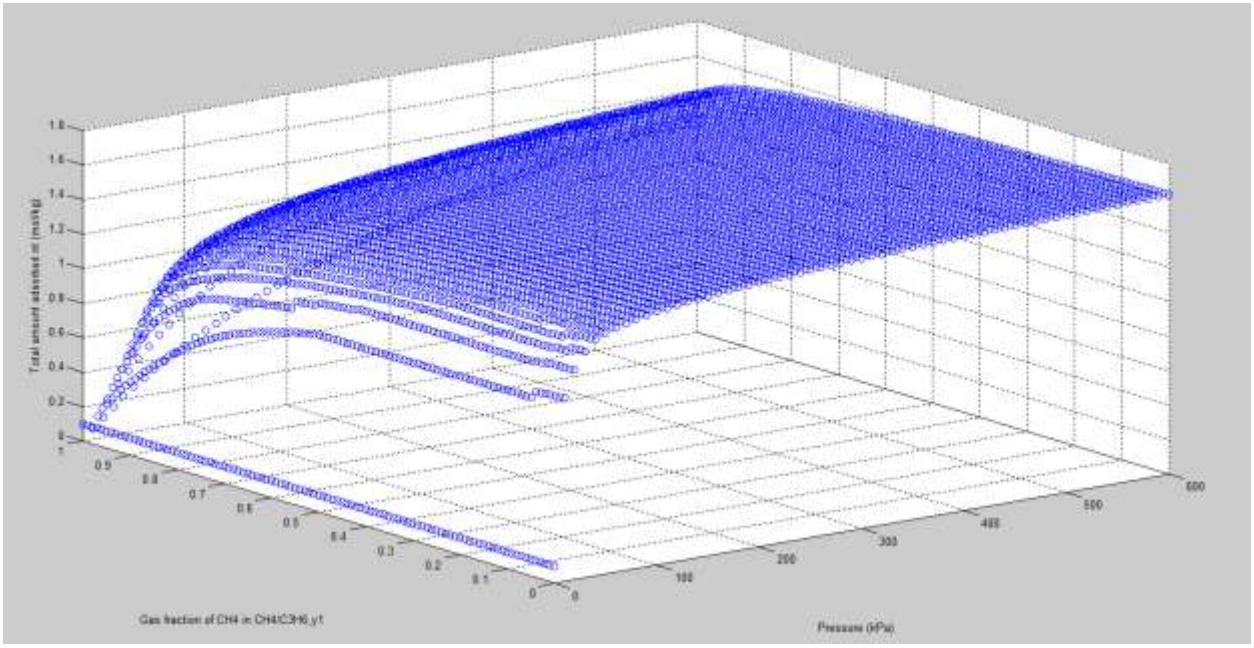

Figure 4.22 Total amount adsorbed for CH4/C3H6 mixture in fraction of pressure and gas composition

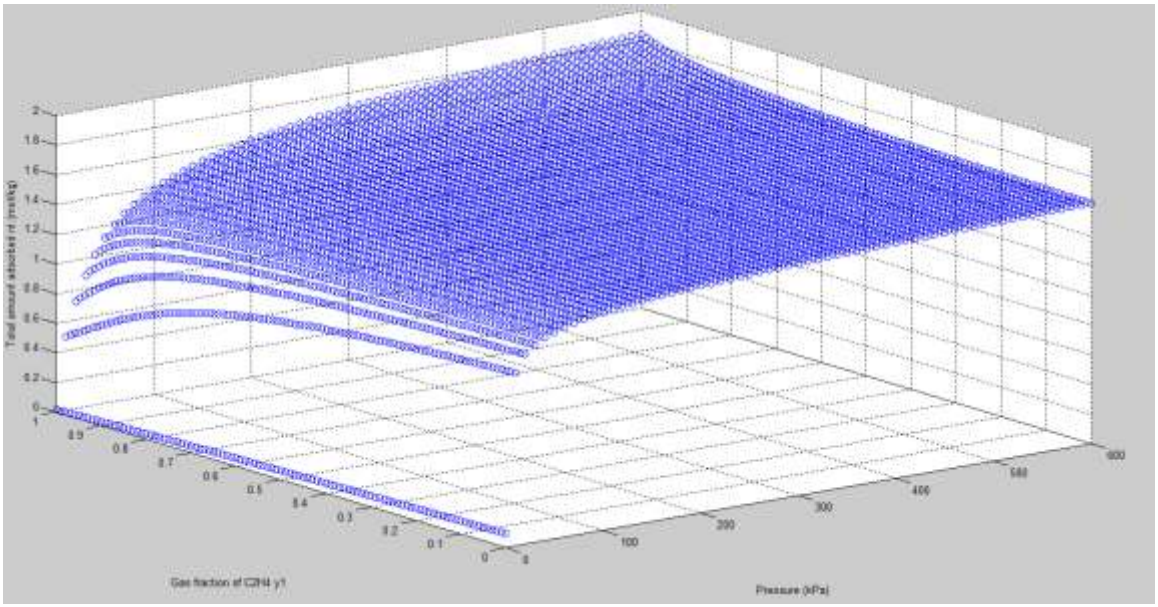

Figure 4.23 Predicted binary isotherms from the Virial-IAST model for C2H4/C3H6 in silicalite.

These 3-D graphs present the predicted total amount adsorbed in binary isotherm adsorption systems. At the end of the compositions, such as y1 equal to 1.0 or 0, the paths are the pure component isotherms measured experimentally.

b) 3-D plots for Selectivity in binary adsorption predictions

Selectivity, acts as a sensitive indicator of phase behavior in adsorption system for practical applications, is also studied in this work. Adsorption separation factor is defined as

$$\alpha_{1,2} = \frac{x1/y1}{x2/y2} = \frac{n1/y1}{n2/y2} \tag{4-1}$$

Where x1, x2, y1 and y2 are the mole fractions and gas fractions of components 1 and 2. n1 and n2 are the amount adsorbed of components 1 and 2 in adsorbed phase.

As a measure of the preference of the adsorbent for component 1 over 2 in different condition, the selectivity of each binary system should approach to the ratio of the two pure components Henry's constant [Talu and Myers, 1988] as pressure approach zero, in thermodynamics.

$$\lim_{P\to 0} \alpha_{1,2} = \frac{K1}{K2} \tag{4-2}$$

For selectivity calculated in this work, the component 1 is always the 'heavy' component in numerator, so that $\alpha_{1,2} > 1.0$.

The effects of total pressure and gas composition on selectivity are shown in Figure 4.24 through 4.29. E.g. Figure 4.24 is the selectivity for CO2/CH4 mixture in silicalite at 35°C.

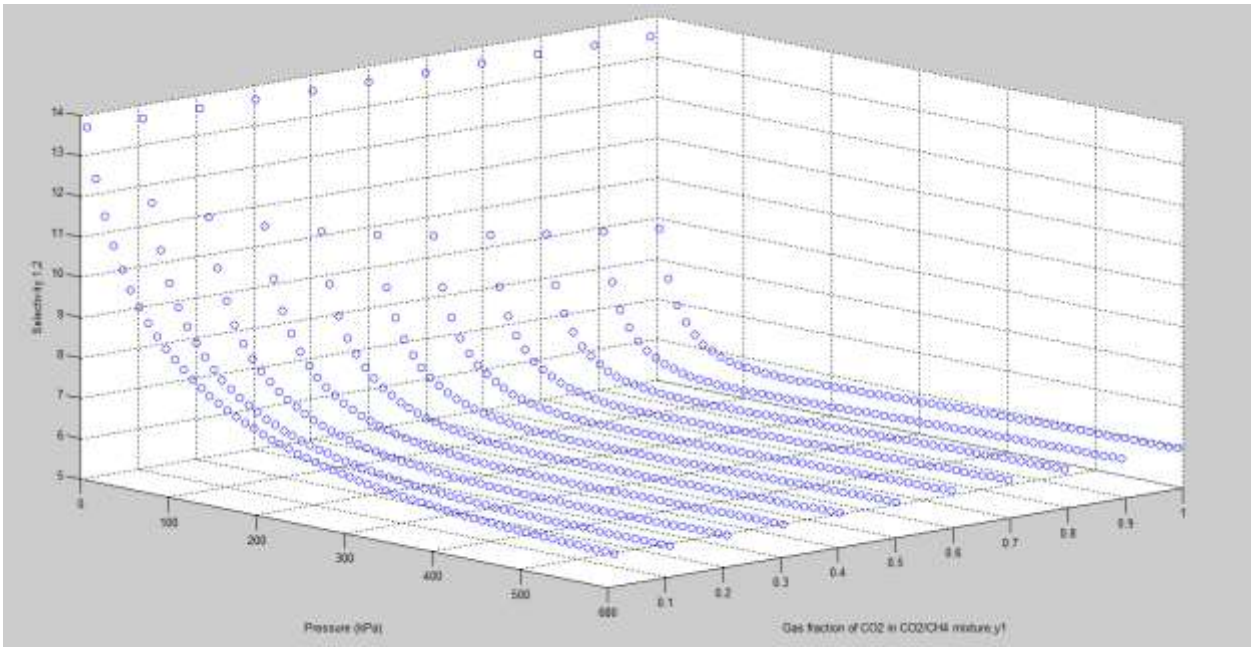

Figure 4.24 Selectivity for CO2/CH4 mixture in fraction of pressure and gas composition

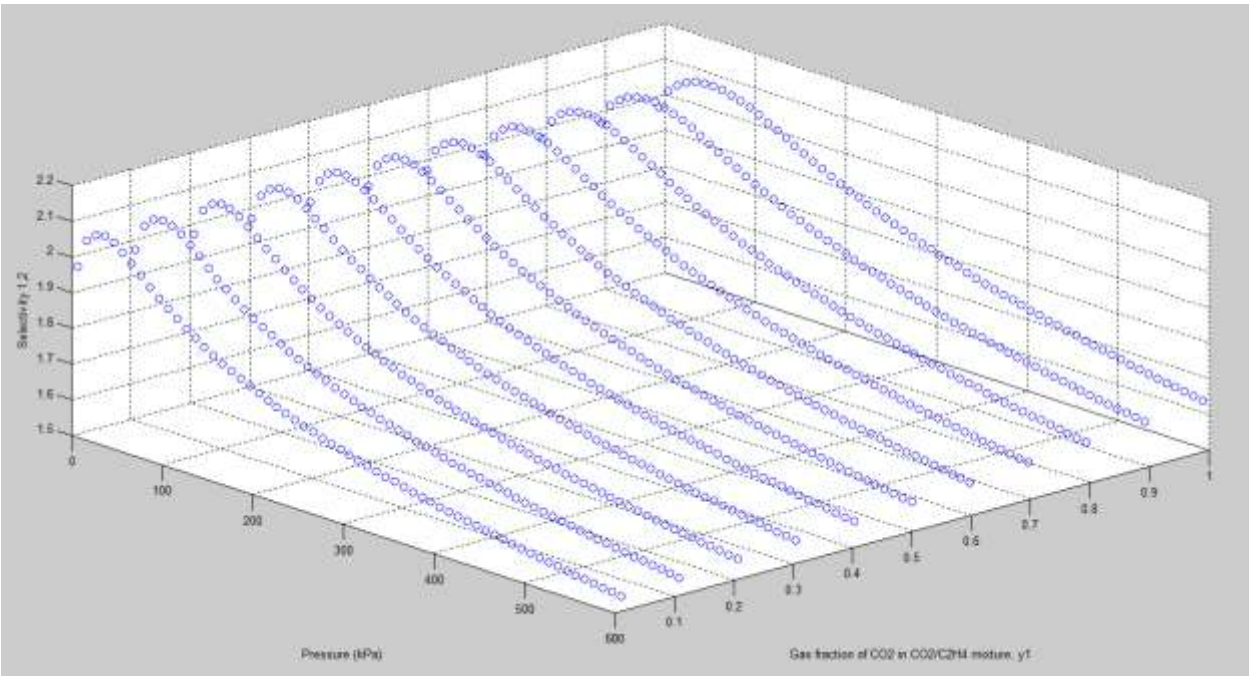

Figure 4.25 Selectivity for CO2/C2H4 mixture in fraction of pressure and gas composition

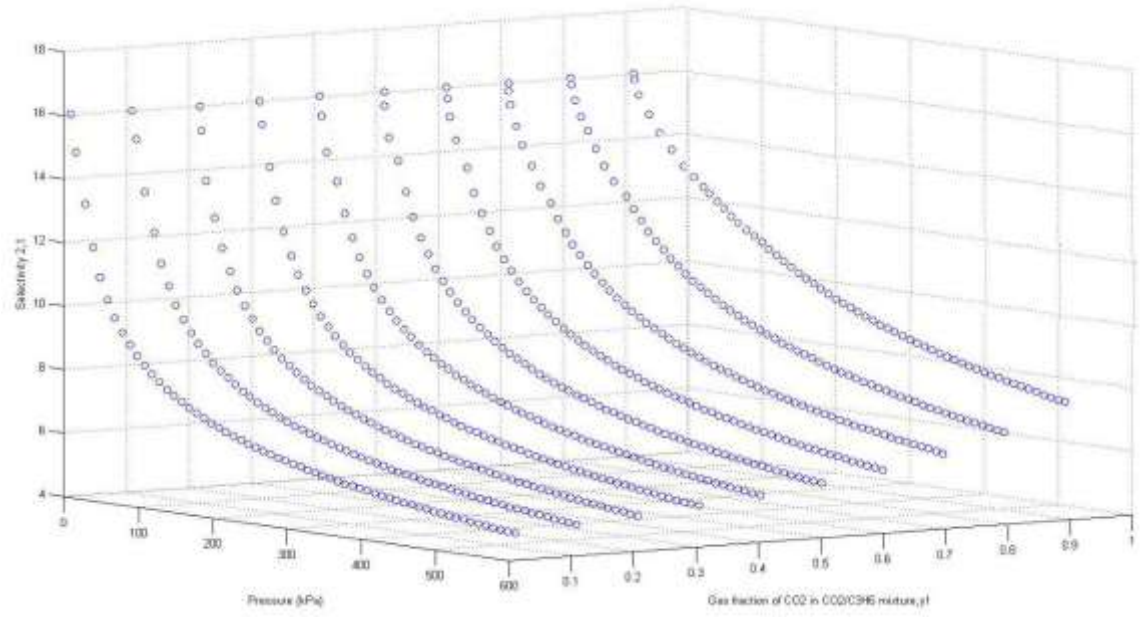

Figure 4.26 Selectivity for CO2/C3H6 mixture in fraction of pressure and gas composition

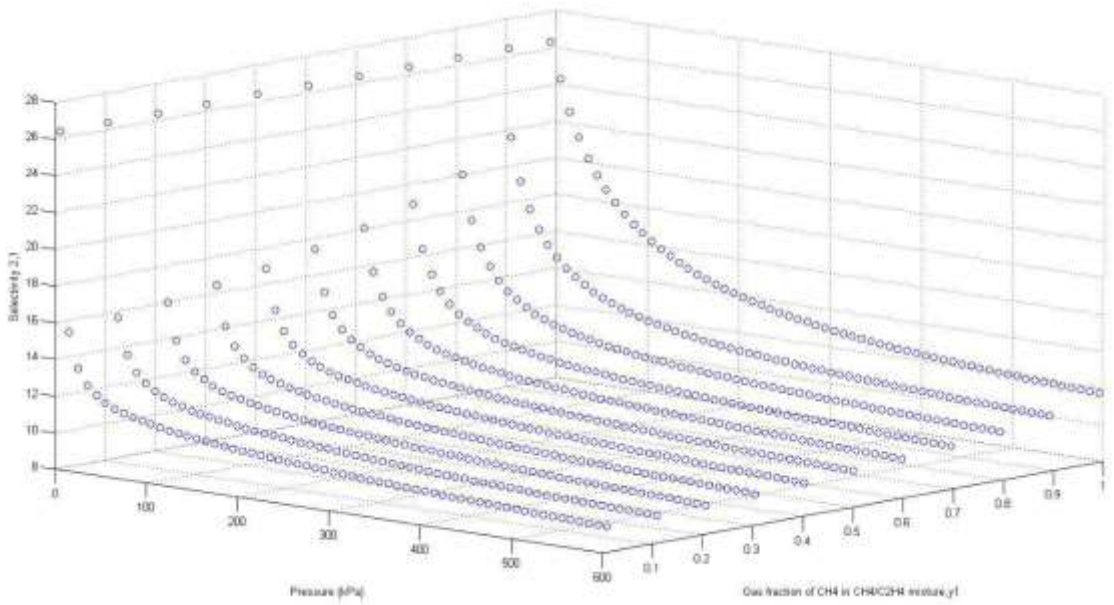

Figure 4.27 Selectivity for CH4/C2H4 mixture in fraction of pressure and gas composition

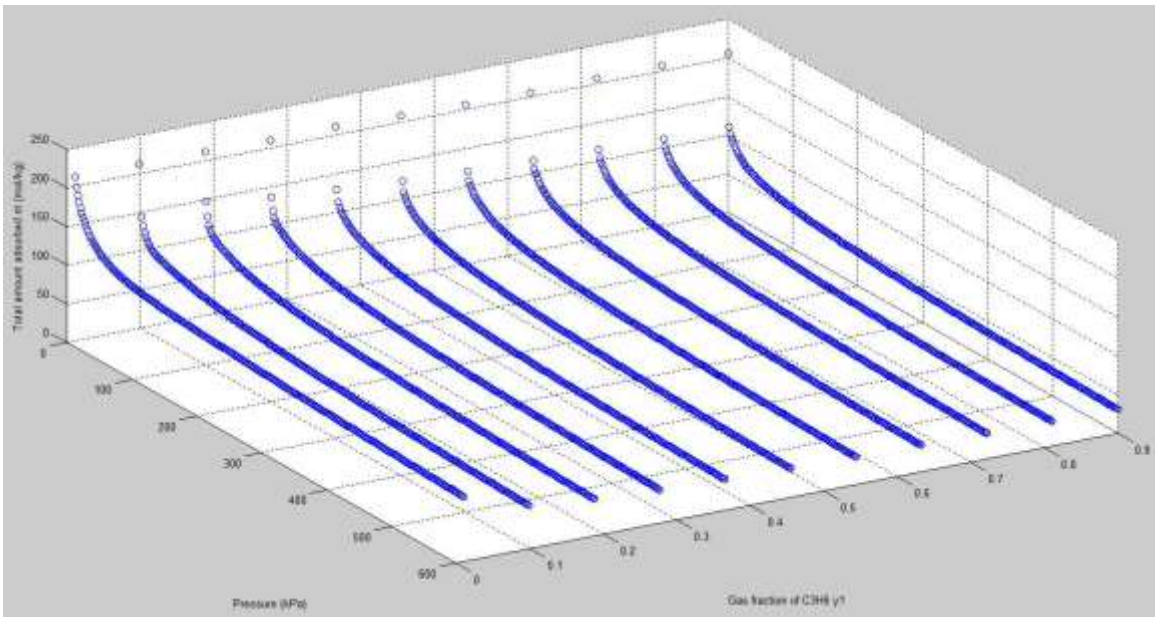

Figure 4.28 Selectivity for C3H6/CH4 mixture in fraction of pressure and gas composition

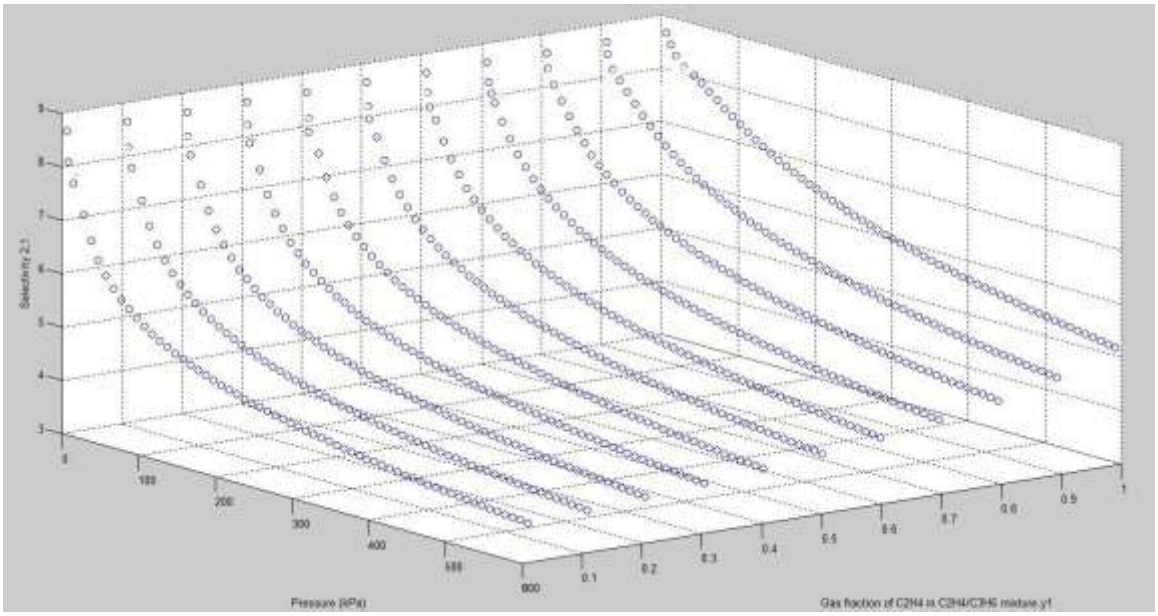

Figure 4.29 Selectivity for C2H4/C3H6 mixture in fraction of pressure and gas composition

In the above Figure 4.24 to 4.29, for each diagram, the selectivity approaches to a constant value at zero pressure. These constant values are equal to the ratio of the pure component Henry's constants for each system.

c) 2-D plots for total amount adsorbed

3-D plots are useful to visualize the phase equilibrium but not very convenient to quantify it. Therefore, 2-D plots are examined to elucidate the effect of pressure, or gas composition, or temperature individually. In this work, temperature is kept constant at 35 C. Effect of pressure is examined at 50:50 mixture and the effect of gas composition is studied under the highest pressure of the light species in each binary system, which are given in Table VIII.

TABLE VIII. Highest pressure of light species for each binary system

Light Species	Highest_P (kPa)	Binary System		
CH4	632	CO2/CH4	-	
C3H6	304	CO2/C3H6	CH4/C3H6	C2H4/C3H6
C2H4	629	CO2/C2H4	CH4/C2H4	-

i) The effect of total pressure

The effect of pressure on total amount adsorbed is studied for 50:50 gas-phase mixtures at 35 C. Figure 4.30 presents predicted total amount adsorbed for mixtures as a function of total pressure. In this figure, C2H4/C3H6 loading is not shown for clarity because it is almost identical to the CO2/C3H6 mixture.

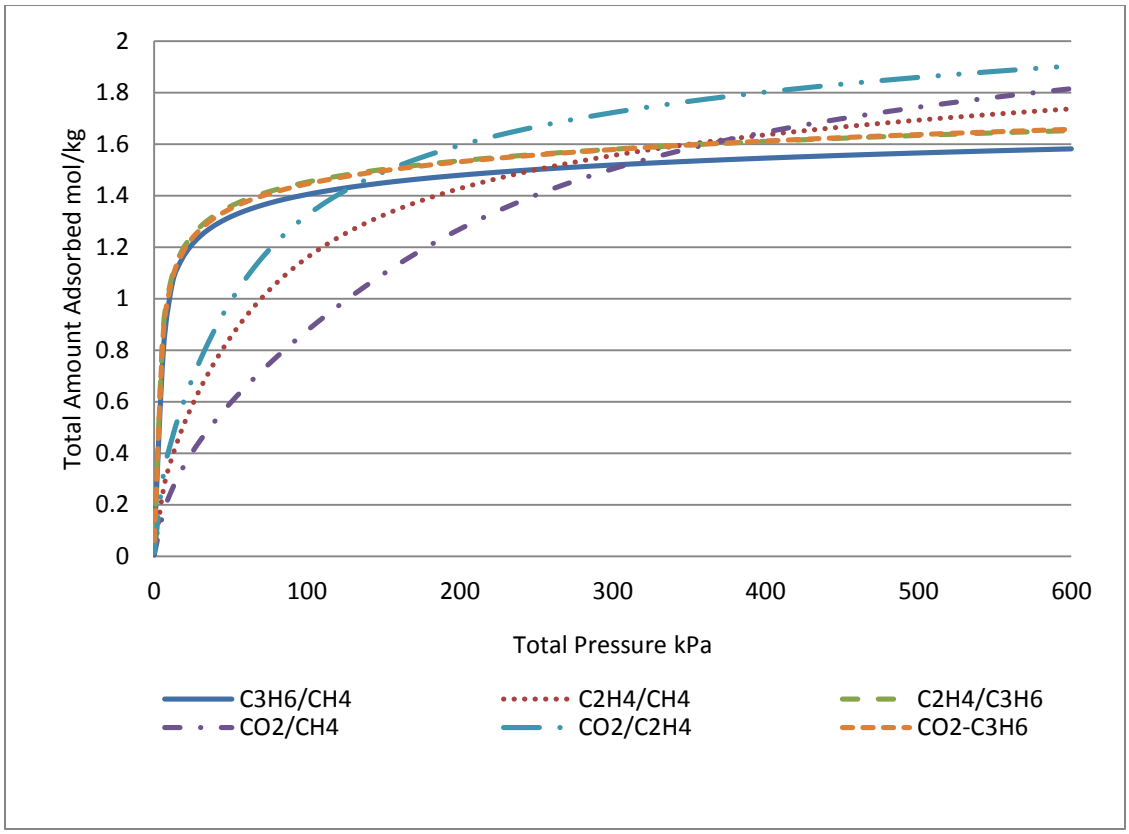

Figure 4.30 Total mount adsorbed for 50:50 gas-phase mixtures in equilibrium

The total amount adsorbed for binary mixtures in low pressure area, 0-100kPa, increase rapidly and tend to reach a plateau at high pressure level. However, without having the experimental data to be compared, the accuracy of binary predictions could not be determined.

ii) The effects of gas composition

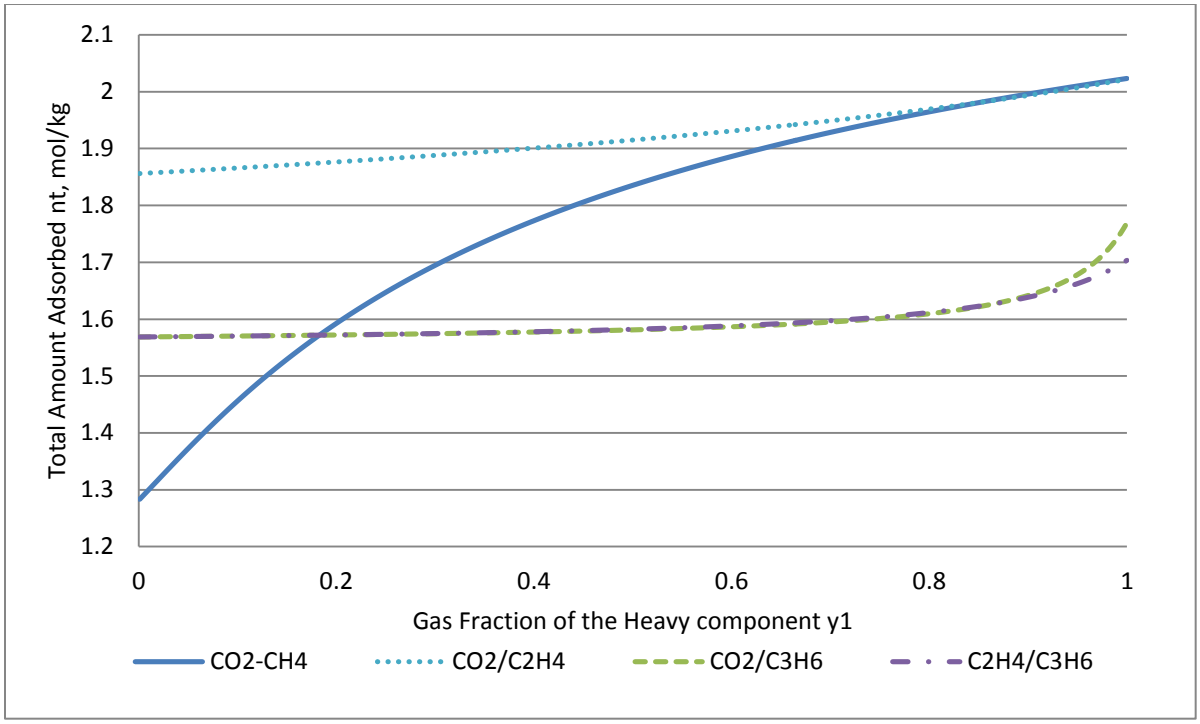

Figure 4.31 Total amount adsorbed for mixtures, CO2/CH4, CO2/C2H4,CO2/C3H6 and C2H4/C3H6 at the highest pressure of the lighter species in each binary system

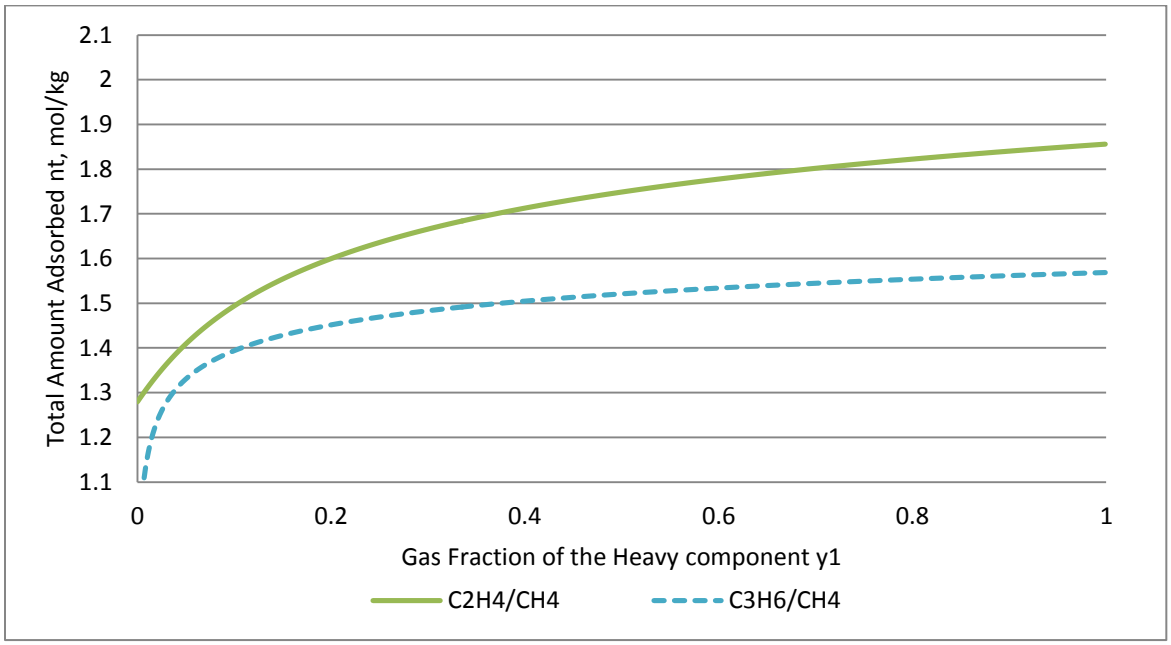

Figure 4.32 Total amount adsorbed for mixtures, CH4/C2H4 and CH4/C3H6 at the highest pressure of the lighter species in each binary system

Total amount adsorbed is predicted as a function of gas composition in above two figures. Figure 4.31 showing an overall increasing tendency which is reasonable since y1 is the gas fraction for the heavy component. Which caused a heavier total amount adsorbed when y1 approach to 1.0.

iii) The effect of temperature

The heat of adsorption will cause significant temperature variations in processes. Thus, the impact of temperature is also important to understand in adsorption phenomena [12].

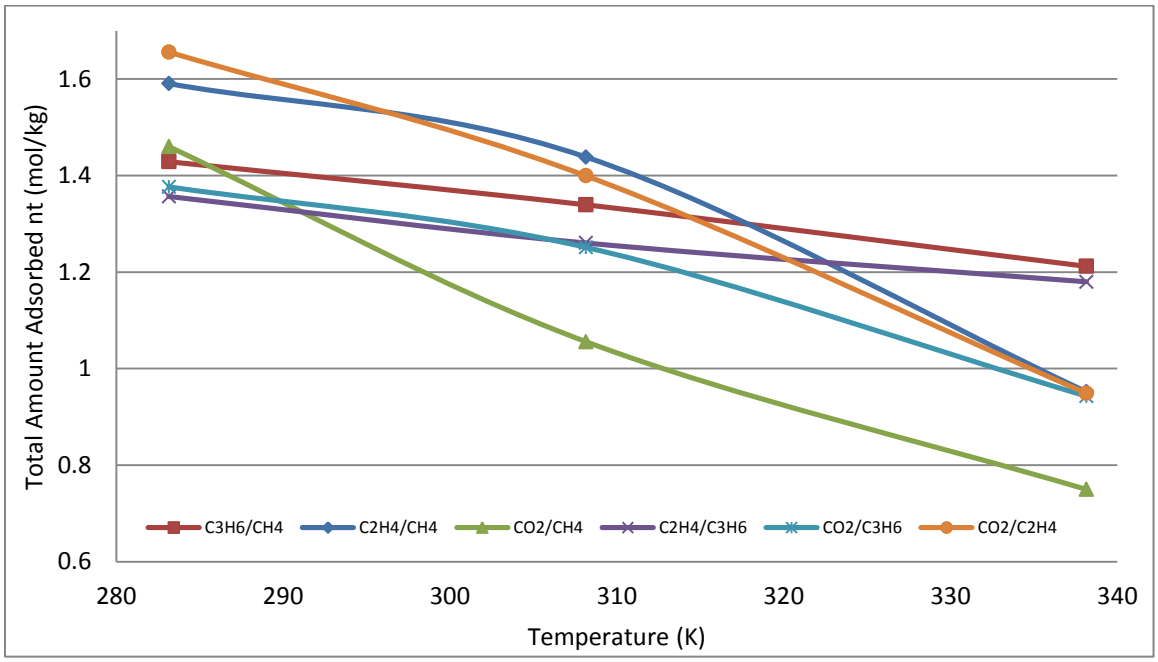

Figure 4.33 Total mount adsorbed for binary mixtures at three different temperatures under each highest pressure of the light species

Figure 4.33 shows that a relatively small temperature change (30K) will cause the total amount adsorbed to change by 32.6% for CO2/CH4 mixture.

d) 2-D plots for selectivity

The selectivity as an important indicator of the phase behavior is studied in below

i) The effects of pressure

In the 50:50 binary adsorption predictions, y1 equals to 0.5, thus the definition of adsorption separation factor

$$\alpha_{1,2} = \frac{x1/y1}{x2/y2} = \frac{n1/y1}{n2/y2} \quad (4\text{-}1)$$

Could be simplified to,

$$\alpha_{1,2} = \frac{x1}{x2} \quad (4\text{-}3)$$

The effect of pressure on selectivity is shown in Figure 4.34. Each prediction approaches a different limiting selectivity above 1.0. The limiting selectivity is same to the ratio of the binary Henry's constant at zero pressure. E.g. the binary prediction approaches a limiting selectivity of 1.869 at zero pressure for CO2/C2H4 mixture while is same to the ratio of the Henry's constant.

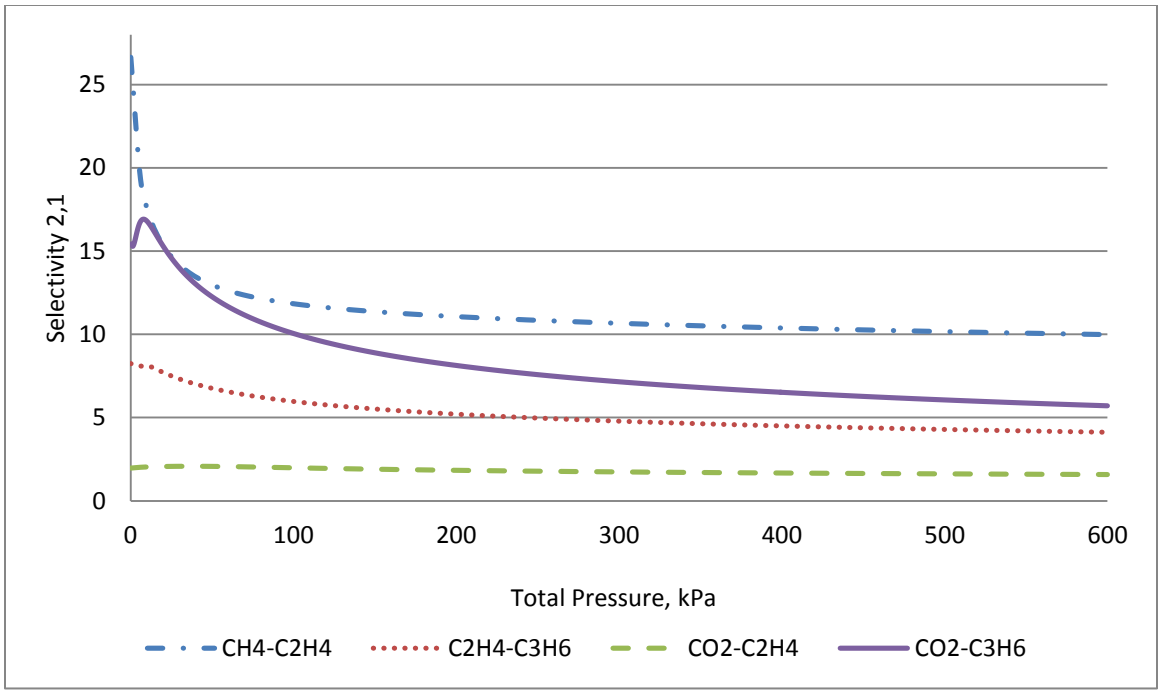

Figure 4.34 Selectivity for 50:50 gas-phase mixtures CH4/C2H4, C2H4/C3H6, CO2/C2H4 and CO2/C3H6 in equilibrium

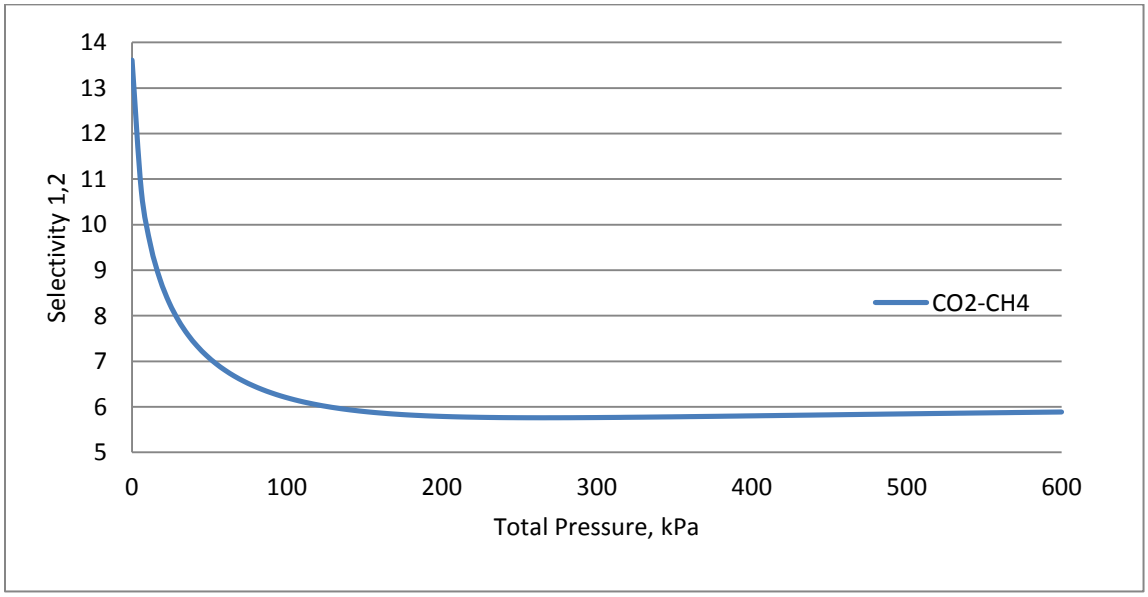

Figure 4.35 Selectivity for 50:50 gas-phase CO2/CH4 mixture in equilibrium

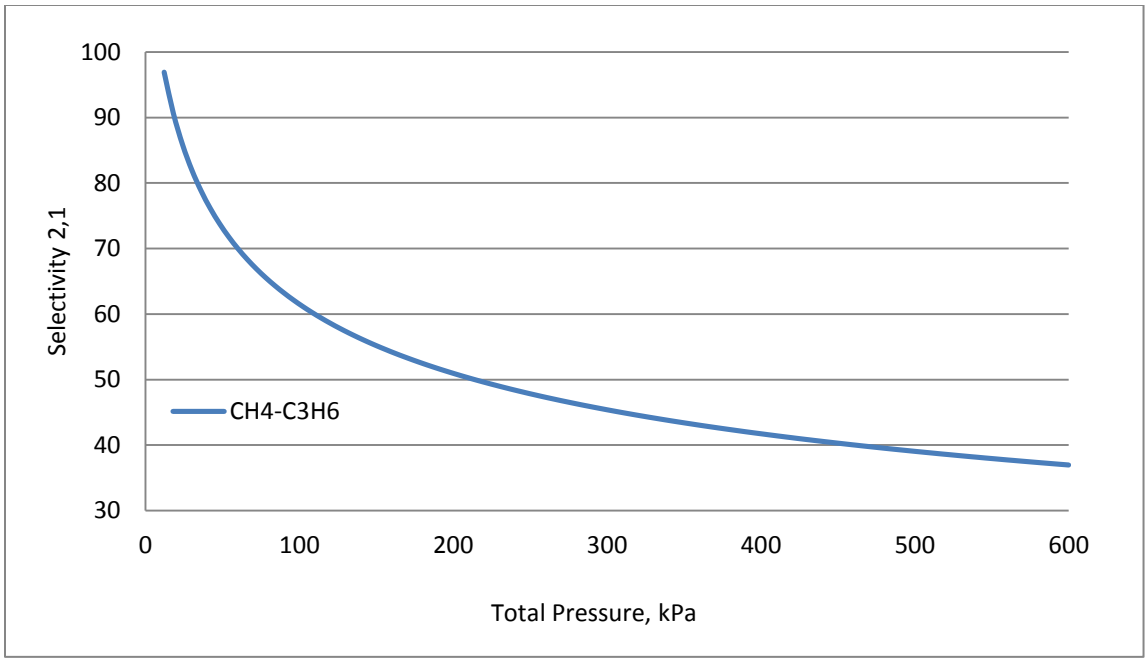

Figure 4.36 Selectivity for 50:50 gas-phase CH4/C3H6 mixture in equilibrium

In Figure 4.36, the selectivity for CH4/C3H6 mixture is suspiciously high than it should be. This may be caused by the inaccurate Henry's constant of C3H6 determined from the pure component isotherm data.

The selectivity diagram is an effective, sensitive way to present the phase behavior and highly sensitive to the Henry's constant.

ii) The effects of gas composition

Figure 4.37 through 4.39 are the variations of selectivity with gas phase composition at highest pressure of lighter species

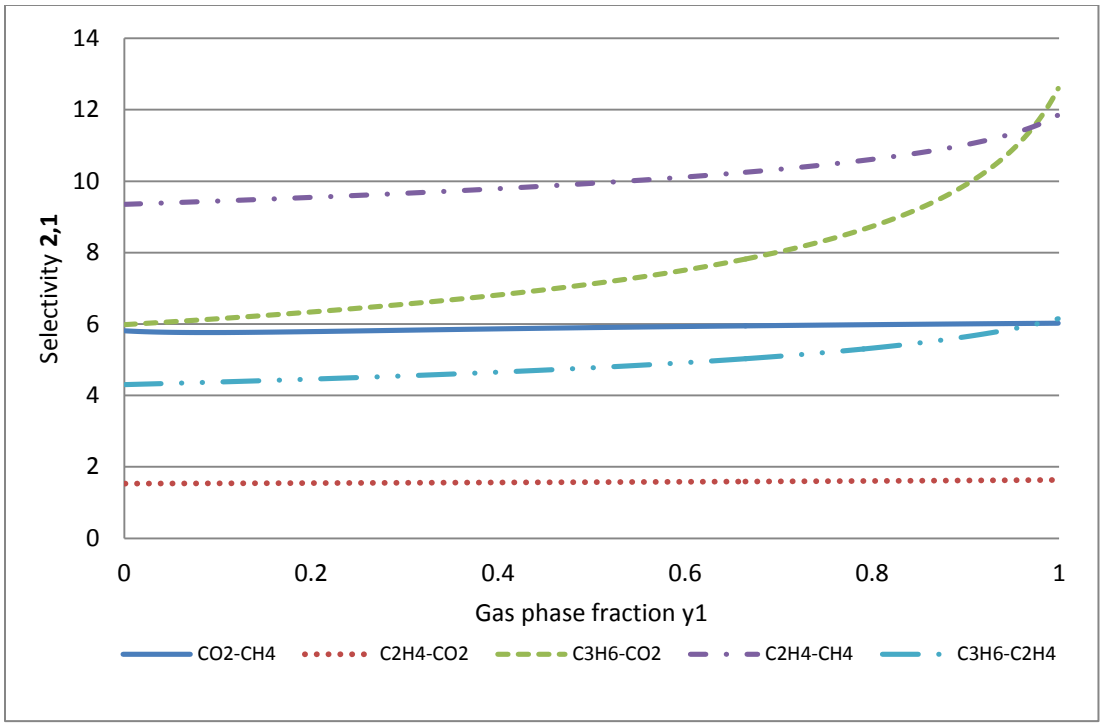

Figure 4.37 Selectivity for binary mixtures at the highest pressure of the lighter species in each system

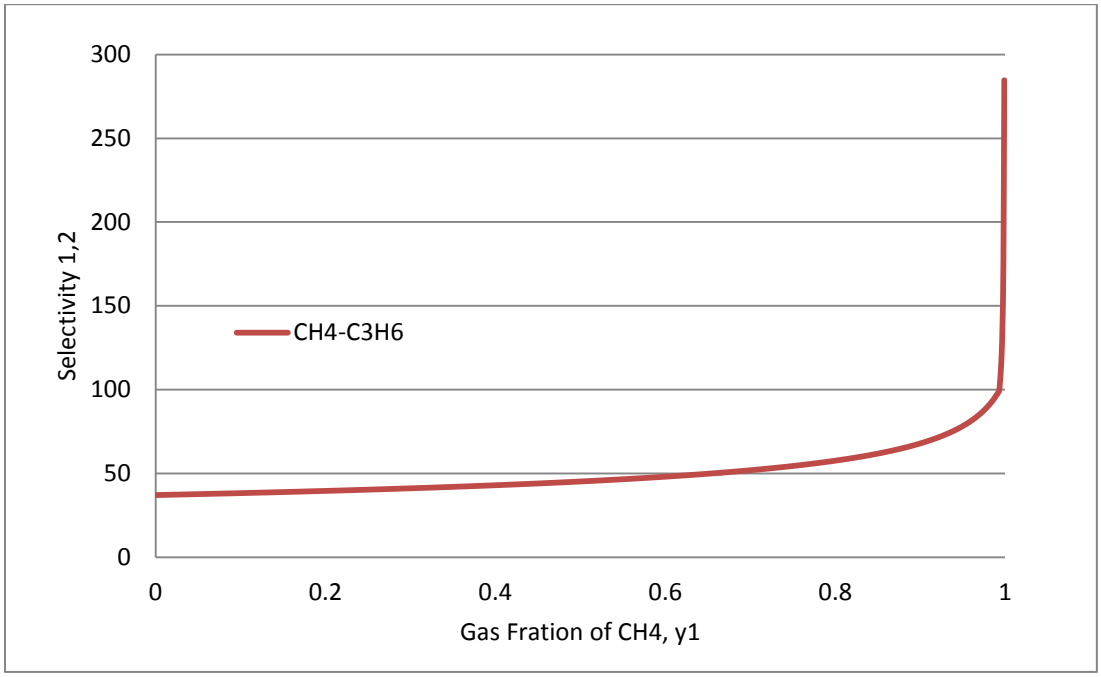

Figure 4.38 Selectivity for binary mixtures at the highest pressure of the light species

In Figure 4.38, the simulation involve C3H6 is showing stability problems again.

iii) The effect of temperature

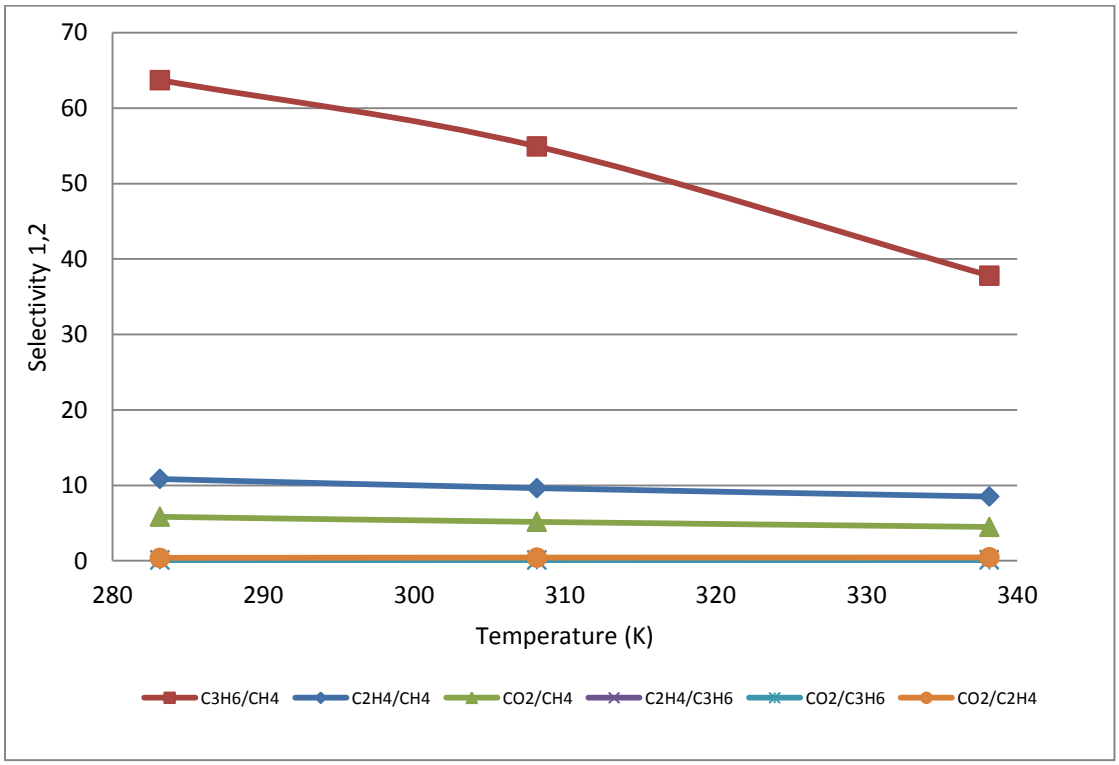

Figure 4.39 Selectivity for binary mixtures at three different temperatures under each highest pressure of the lighter species

In the conditions studied (629 kPa and y1=0.5), the effect of temperature on selectivity is small, as indicated in Figure 4.39.

CHAPTER V

SUMMARY AND CONCLUSIONS

In this section the analysis of all pure component experiments are presented first, followed by predictions of binary phase equilibrium.

A. Pure Component Adsorption Isotherms

Pure component adsorption isotherms of methane, ethylene, propylene and carbon dioxide were obtained volumetrically at three different temperatures, as 10C, 35C and 65C.

For these four gases studied, the saturation capacities are in the order CO2>CH4>C2H4>C3H6. Although the CH4 isotherms did not reach high enough plateau pressure levels, this order can be deduced from considering data and molecular sizes.

Henry's constant plays a significant role in adsorption thermodynamics while modeling the adsorption isotherm equilibrium. It is the slope at origin of the isotherms. According

to the comparison of the slopes under same temperature for four gases, the order of Henry's constant is C3H6>C2H4>CO2>CH4.

The pure component adsorption data are modeled by Virial model and Langmuir model. The Virial model with three parameters represents the dataset more accurately than Langmuir model in this study. Furthermore, the Virial model outperforms greatly following the data at low pressure. It is found to be a reliable way to calculate the Henry's law constants with good accuracy.

The Virial isotherm equation with T-independent parameters is used in the binary predictions with IAST model.

B. Binary Adsorption Phase Equilibrium

Even the simplest multicomponent, binary adsorption measurement is complicated and time- consuming, due to the extra degree of thermodynamic freedom in adsorption. Hence, the binary predictions are made by IAST-Virial model, based on the obtained temperature independent parameters of pure component adsorptions. This method is quite straightforward and time-saving for an initial assessment of binary phase behavior.

Matlab Software is used in this study to handle the numerous calculations, by solving related non-linear equations, to predict the total amount adsorbed and selectivity in binary system. The accuracy and reliability of IAST-Virial predictions need to be further studied by collecting binary adsorption experimental data from a real detailed analysis.

Binary adsorption of CO2/CH4, CO2/C2H4, CO2/C3H6, CH4/C2H4, CH4/C3H6 and C2H4/C3H6 are predicted at 35C. For all of the mixtures, the total amount adsorbed and selectivity can be successfully predicted using IAST-Virial model. Predictions of binary behavior for binary mixtures are highly sensitive to Henry's constant. For those mixtures including C3H6, the predictions are much less accurate caused by the less accurately determined Henry's Law constant.

REFERENCES

[1]. O.Talu, Needs, status, techniques and problems with binary gas adsorption experiments, Advances in Colloid an Interface Science, 76-77 (1988) 227-269

[2]. Douglas M. Ruthven, Principles of Adsorption and Adsorption Processes, 1984

[3]. Matthew S. Sun, D.B. Shah, Heather H. Xu and Orhan Talu, Adsorption Equilibria of C1 to C4 Alkanes, CO2 and SF6 on Silicalite, J.Phys.Chem. B 1998, 102, 1466-1473

[4]. O. Talu, Measurement and Analysis of Mixture Adsorption Equilibrium in Porous Solids, Chemie Ingenieur Technik, Volume 83, issue 1-2 (January, 2011), p. 67-82

[5]. A.L. Myers, J.M. Prausnitz, AIChE J. 11 (1965) 121.

[6]. R.M. Barrer and J.A. Davies, Proc. Roy. (1970)

[7]. A. L. Myers, Thermodynamics of adsorption in porous materials, A.I.Ch.E. J., 2002, 48, 145–160.

[8]. A.L. Myers, J. Calles, G. Calleja, Adsorption 1997. 3.107

[9]. Myers, A. L.; Prausnitz, J. M. Thermodynamics of mixed-gas adsorption. AIChE J. 1965, 11 (1), 121–127.

[10]. O'Brien, J. A.; Myers, A. L. Rapid calculations of multi-component adsorption equilibria from pure isotherm data. Ind. Eng. Chem. Process Des. Dev. 1985, 24 (4), 1188–1191.

[11]. Database of Zeolite Structures.

[12]. Orhan Talu, Jianmin Li, Measurement and analysis of oxygen/nitrogen/ 5A-zeolite adsorption equilibria for air separati Gas Sep. Purif. 1996

APPENDIX A

PURE COMPONENT ADSORPTION DATA

TABLE IX Experimental Adsorption Isotherm Data

T = 10C		T = 35C		T = 65C	
P (kPa)	N (mol/kg)	P (kPa)	N (mol/kg)	P (kPa)	N (mol/kg)
Methane					
5.861	0.0755	9.757	0.0615	9.964	0.0303
12.34	0.1470	18.72	0.1120	13.27	0.0401
22.31	0.2424	32.92	0.1841	23.65	0.0700
34.48	0.3443	37.13	0.2051	50.82	0.1430
46.09	0.4282	51.40	0.2684	71.57	0.1897
48.23	0.4415	57.16	0.2938	79.29	0.2130
70.12	0.5776	153.8	0.6141	115.8	0.2930
116.9	0.7963	254.1	0.8363	148.2	0.3514
198.9	1.0443	394.8	1.0506	219.3	0.4824
273.4	1.1927	437.5	1.1141	257.2	0.5351
326.1	1.2874	621.9	1.2754	384.8	0.7167
562.6	1.5009	633.0	1.2871	557.8	0.8906
Ethylene					
1.758	0.3170	0.758	0.0904	2.172	0.1135
5.240	0.6140	2.103	0.1747	7.516	0.2205
10.38	0.8905	3.310	0.2512	13.82	0.3203
18.79	1.1428	5.895	0.3567	22.75	0.4400
30.48	1.3233	7.171	0.3855	38.54	0.6081
48.03	1.4700	8.964	0.4627	56.13	0.7523
68.95	1.5672	11.65	0.5442	96.53	0.9794
72.05	1.5602	12.31	0.5580	141.4	1.1309
91.71	1.6410	16.24	0.6529	180.0	1.2249
141.4	1.7368	20.20	0.7341	238.9	1.3265
190.7	1.8007	24.48	0.8114	289.6	1.3990
192.7	1.7748	34.10	0.9710	398.9	1.5054
293.7	1.8798	67.99	1.2503	512.0	1.5885
325.8	1.8692	88.60	1.3350	583.7	1.6054
404.1	1.9331	111.0	1.4222	656.8	1.6707
435.8	1.9110	164.1	1.5315	670.2	1.6510
546.8	1.9437	236.9	1.6173		
660.9	1.9727	242.7	1.6344		
		322.0	1.7047		
		374.8	1.7255		
		438.2	1.7759		
		556.8	1.8351		
		629.5	1.8384		

TABLE IX (Continued)

T = 10C		T = 35C		T = 65C	
P (kPa)	N (mol/kg)	P (kPa)	N (mol/kg)	P (kPa)	N (mol/kg)
Propylene					
		0.138	0.1201	0.586	0.1307
		0.448	0.1355	0.827	0.1651
		0.517	0.3162	3.344	0.4405
		1.827	0.7177	5.964	0.6455
		1.862	0.4618	6.033	0.6117
		4.861	0.9004	7.274	0.7062
		12.27	1.2148	12.03	0.9000
		28.58	1.3709	38.72	1.1984
		53.06	1.4407	57.64	1.2750
		120.7	1.4787	81.36	1.3186
		172.7	1.5095	84.81	1.3446
		304.4	1.5334	90.81	1.3445
				146.2	1.4195
				152.4	1.4320
				239.3	1.4457
				268.6	1.4877
				453.7	1.5404
				455.1	1.5192
				654.0	1.5712
Carbon Dioxide					
0.621	0.1271	1.655	0.1181	3.551	0.0930
2.551	0.2499	6.240	0.2392	3.551	0.0930
4.413	0.3339	6.999	0.2562	3.654	0.0923
5.551	0.3810	12.51	0.3556	9.481	0.1646
5.723	0.3114	11.48	0.2758	16.31	0.2288
9.964	0.5352	21.00	0.4708	20.41	0.2660
10.76	0.5599	23.51	0.5210	20.41	0.2660
10.93	0.5649	28.96	0.5910	23.62	0.2881
15.38	0.6370	23.65	0.4594	31.41	0.3450
18.51	0.7802	43.27	0.6892	37.51	0.3867
20.27	0.8187	87.57	1.0506	39.20	0.3970
28.34	0.9920	97.91	1.1562	50.89	0.4725
31.72	1.0577	113.8	1.1954	50.89	0.4725
32.30	1.0621	135.1	1.2848	59.61	0.5192
36.34	1.0881	164.5	1.4493	81.29	0.6323
37.17	0.8974	181.0	1.5358	81.29	0.6336
40.79	1.1967	178.6	1.4972	81.81	0.6345
41.03	1.2039	210.0	1.5783	107.6	0.7498
46.54	1.2451	211.7	1.5843	107.6	0.7498

TABLE IX (Continued)

T = 10C		T = 35C		T = 65C	
P (kPa)	N (mol/kg)	P (kPa)	N (mol/kg)	P (kPa)	N (mol/kg)
Carbon Dioxide					
54.16	1.3608	271.7	1.7280	109.6	0.7604
62.06	1.4107	426.1	1.9155	109.6	0.7604
65.85	1.4187	433.0	1.9020	109.6	0.7617
67.68	1.4826	637.1	2.0499	110.3	0.7598
71.71	1.5066			121.0	0.8049
74.19	1.5336			168.6	0.9764
86.53	1.6174			220.0	1.1057
87.91	1.5494			231.0	1.1426
93.77	1.6397			281.7	1.2439
113.4	1.6419			291.3	1.2702
118.3	1.7613			300.3	1.2902
147.6	1.8560			338.6	1.3437
170.0	1.9639			410.3	1.4553
173.8	1.8616			428.9	1.4720
218.9	2.0269			602.0	1.6544
255.8	2.0586			627.5	1.6806
307.2	2.0962				
353.4	2.1926				
405.4	2.1807				
440.9	2.1995				
587.8	2.3061				

APPENDIX B

MATLAB PROGRAM CODE FOR BINARY ADSOPRTION PREDICTION

```
% qianqian01_f
%
%   function for IAST
%   QianQian Zhou
function F = qianqian01_f(x)
global y1 P k b c d
% recover parameters

k1 = k(1);
k2 = k(2);
b1 = b(1);
b2 = b(2);
c1 = c(1);
c2 = c(2);
d1 = d(1);
d2 = d(2);

% initialize
F = zeros(size(x));
% recover variables
x1 = x(1);
x2 = 1 - x1;

n1o = x(2);
n2o = x(3);
```

```
P1o = x(4);

P2o = x(5);

F(1) = y1 - x1*P1o/P;

F(2) =(1-y1)-(1-x1)*P2o/P;

e1 = k1 + b1*n1o + c1*n1o^2+ d1*n1o^3;

F(3) = P1o - n1o * exp(e1);


e2 = k2 + b2*n2o + c2*n2o^2+ d2*n2o^3;

F(4) = P2o - n2o * exp(e2);

ee1 = n1o + b1/2 * n1o^2 +2*c1/3 * n1o^3 +3*d1/4 * n1o^4;

ee2 = n2o + b2/2 * n2o^2 +2*c2/3 * n2o^3 +3*d2/4 * n2o^4;

F(5) = ee1 - ee2;

return

>>>>>>>>>>>>>>>>>>

% qianqian01.m

Clear  % clear screen

clc

% transfer parameters

global y1 P k b c d


fprintf ('\n *** Ideal Adsorbed Solution Theory *** \n');


k1=2.404;    % carbon dioxide--35C

b1=3.961;

c1=-2.902;
```

```
d1=0.87;

k2=5.022;      % CH4--35C,

b2=0.98;

c2=-0.457;

d2=0.32;

 % set parameters

k = [k1; k2];

b = [b1; b2];

c = [c1; c2];

d = [d1; d2];

% set known conditions

y1 = 0.01; % an initial value

P  = 0.1; % just an initial value

% set problem

fun = 'qianqian01_f';

n1o = 0.01;

n2o = 0.1;

x1 = 0.01;

x2 = 1 - x1;

P1o = 10;

P2o = 1;

% set initial guess

x0 = [x1; n1o; n2o; P1o; P2o];

% % uncomment to check !

% F0 = feval(fun, x0)
```

```
% Fnorm = norm(F0)

options =optimset('Display','off');

% solve for a given y1 value

y1_initial = y1;

y1_final = 1.0;

y1_values = linspace (y1_initial, y1_final, 11)';

% solve for a given P value

P_initial = P;

P_final = 600;

P_values = linspace (P_initial, P_final, 61)';

% initialize

Results = [];

for e = 1:1:length(y1_values)

      y1=y1_values(e);

   for counter = 1:1:length(P_values)

P = P_values(counter);

x = fsolve (fun, x0, options);

F = feval(fun, x);

Fnorm = norm(F);

% recover variables

x1 = x(1);

x2 = 1-x1;

n1o = x(2);

n2o = x(3);

P1o = x(4);
```

```
P2o = x(5);

% total amount adsorbed

nt= n1o*n2o/(x1*n2o+x2*n1o);

% % selectivity

% s= x1*(1-y1)/(x2*y1);  % s1,2

% s= (x2*y1)/x1*(1-y1);  % s2,1

Results = [Results;    P, y1, nt, x1, n1o, P1o, x2, n2o, P2o, Fnorm];

% reset initial condition

x0 = x;

end

x0=[0.01;0.1;0.1;10;1];  % the initial assumption

end

display (Results);

x=Results(:,1);y=Results(:,2);z=Results(:,3);

scatter3(x,y,z) % 3-D scatter plot

xlabel('Pressure (kPa)')

ylabel ('Gas fraction of CO2 y1')

zlabel('Total amount adsorbed nt (mol/kg)')
```